EFFECTS OF TRIMETHYLAMINE N-OXIDE ON MOUSE EMBRYONIC STEM CELL PROPERTIES

Catherine M. Barron

Thesis submitted to the faculty of the Virginia Polytechnic Institute and State University in partial fulfillment of the requirements for the degree of

Master of Science

In

Biomedical and Veterinary Sciences

Jia-Qiang He (Chair)

Willard Eyestone

Robert Gourdie

Dongmin Liu

July 14, 2020

Blacksburg, VA

Keywords: Trimethylamine N-oxide, mouse embryonic stem cells, pluripotency, metabolism, mitochondria, reactive oxygen species, proton leak

Effects of Trimethylamine N-Oxide on Mouse Embryonic Stem Cell Properties

Catherine M. Barron

ACADEMIC ABSTRACT

Trimethylamine N-oxide (TMAO) is a metabolite derived from dietary choline, betaine, and carnitine via intestinal microbiota metabolism. In several recent studies, TMAO has been shown to directly induce inflammation and reactive oxygen species (ROS) generation in numerous cell types, resulting in cell dysfunction. However, whether TMAO will impact stem cell properties remains unknown. This project aims to explore the potential impact of TMAO on mouse embryonic stem cells (mESCs), which serve as an in vitro model of the early embryo and of other potent stem cell types. Briefly, mESCs were cultured in the absence (0mM) or presence of TMAO under two different sets of treatment conditions: long-term (21 days), low-dose (20μM, 200μM, and 1000μM) treatment or short-term (5 days), high-dose (5mM, 10mM, 15mM) treatment. Under these treatment conditions, mESC viability, proliferation, and stemness were analyzed. mESC properties were not negatively impacted under long-term, low-dose TMAO treatment; however, short-term, high-dose treatment resulted in significant reduction of mESC viability and proliferation. Additionally, mESC stemness was significantly reduced when high-dose treatment was extended to 21 days. To investigate an underlying cause for TMAO-induced loss in mESC stemness, metabolic activity of the mESCs under short-term, high-dose TMAO treatment was measured with a Seahorse XFe96 Analyzer. TMAO treatment significantly decreased the rate of glycolysis, and it increased the rate of compensatory glycolysis upon inhibition of oxidative phosphorylation (OxPHOS). It also significantly increased the rate of OxPHOS, maximal respiratory capacity, and respiratory reserve. These

findings indicate that TMAO induced a metabolic switch of mESCs from high glycolytic activity to greater OxPHOS activity to promote mESC differentiation. Additionally, TMAO resulted in increased proton leak, indicating increased oxidative stress, and elucidating a potential underlying mechanism for TMAO-induced loss in mESC stemness. Altogether, these findings indicate that TMAO decreases stem cell potency potentially via modulation of metabolic activity.

Effects of Trimethylamine N-Oxide on Mouse Embryonic Stem Cell Properties

Catherine M. Barron

GENERAL AUDIENCE ABSTRACT

Trimethylamine N-oxide (TMAO) is a metabolite that is produced by the bacteria in the gut after the consumption of specific dietary ingredients (e.g., choline, carnitine, betaine). These ingredients are commonly found in meat and dairy products, and thus make up a large part of the average American diet. Recently, it was discovered that high TMAO levels in the bloodstream put people at an increased risk for heart disease, neurodegenerative diseases (e.g., Alzheimer's Disease), diabetes, stroke, and chronic kidney disease. At the cellular level, there is evidence that TMAO increases inflammation and the production of oxygen radicals, which causes cells to lose their function and promotes the onset of disease. TMAO has been well studied in adult cell types; however, no one has investigated whether TMAO will impact cells of the early embryo. This project aims to explore the impact of TMAO on mouse embryonic stem cells (mESCs), which are cells that represent the early stage of embryonic development and are critical for proper development of the final offspring. In addition, mESCs may also help to provide insight into how TMAO impacts other stem cell types, some of which are present throughout the entire human lifespan and play an important role in the body's ability to repair itself and maintain overall health. My project demonstrated that TMAO does not impact the overall health of mESCs under normal conditions, which signifies that TMAO generated by a pregnant mother may not directly impact the early embryonic stage of development. Further studies should be conducted to determine the potential impact of TMAO on late stages of embryonic and fetal development. Next, to simulate diseased conditions, the mESCs were treated with extremely

high concentrations of TMAO in order to determine what concentration of TMAO will negatively impact these cells. It was found that at 5mM TMAO, mESCs begin to lose their basic properties and become dysfunctional. They are impaired in their viability, growth, ability to become other cell types, and in their metabolic activity. These mESC properties are shared with several types of adult stem cells, and therefore, these findings help to provide insight into how TMAO may impact stem cells found in the adult body which are exposed to a lifetime of high TMAO levels. In the future, we would like to further explore the impact of TMAO on mESCs at the molecular level as well as examine the direct impact of TMAO on other stem cell types.

DEDICATION

To my grandmother, Elizabeth Morrissey, for being the strongest person I know, and motivating me to keep pushing myself to learn and grow every day.

AKNOWLEDGEMENTS

First, I would like to thank my advisor and mentor, Dr. Jia-Qiang He. Thank you for investing so much time in teaching me and providing me with the opportunity to learn new scientific concepts and skills. I am appreciative of your support over the years and your willingness to help at all times of the day.

Thank you to my committee members, Dr. Will Eyestone, Dr. Robert Gourdie, and Dr. Dongmin Liu for your valuable input and helping to guide me through my project. Thank you for taking the time to attend my committee meetings and challenging my experimental design and analysis. I greatly appreciate your generosity of time.

Thank you to Dr. Brown for allowing me to run metabolic experiments with his Seahorse XFe96 Analyzer, and to his student Grace Davis who ran those experiments.

I would like to thank He lab members past and present, including Benjamin Ledford and Miao Chen who were excellent labmates and taught me a great deal. Thanks to Youjing Zheng, Swagatika Paul, and Ahmet Ceylan for being excellent collaborators and wonderful friends. I also want to thank Nathalie Groot who helped to maintain the cells and perform analysis.

I am also grateful to Dr. Ansar Ahmed, Andrea Green, Monica Taylor, and Dr. Jessica Crawford for being very supportive throughout my time as a graduate student and always being available to answer my questions. And thank you to Allison Price, Andrea Renshaw, Pete Jobst, and Jen Averill as well for your support.

This research would not have been possible without the financial support of the Virginia-Maryland College of Veterinary Medicine (VMCVM) Office of Research and Graduate Studies and NIH. I thank and appreciate these funding supports.

Lastly, I could not have done this without the support of Hani Mustafa, Claire Barron, Donal Barron, Elizabeth Barron, David Barron, and Xavier Cabana-Puig. Thank you to all my friends and family for your encouragement and positivity throughout my graduate studies.

TABLE OF CONTENTS

LIST OF FIGURES

LIST OF ABBREVIATIONS

2-DG	2-Deoxyglucose
2-ME	2-Mercaptoethanol
3-BrPa	3-Bromopyruvate
EdU	5-Ethynyl-2'-Deoxyuridine
PRPP	5-Phosphoribosyl-1-Pyrophosphate
ADP	Adenosine Diphosphate
ATP	Adenosine Triphosphate
AD	Alzheimer's Disease
AMA	Antimycin-A
ANOVA	Analysis of Variance
ATPase	ATP Synthase
ACL	ATP-Citrate Lyase
BSA	Bovine Serum Albumin
FCCP	carbonylcyanide p-trifluoromethoxyphenylhydrazone
CKD	Chronic Kidney Disease
CVD	Cardiovascular Disease
DT	Doubling Time
DMEM	Dulbecco's Modified Essential Medium
ETC	Electron Transport Chain
eNOS	Endothelial Nitric Oxide Synthase
EPCs	Endothelial Progenitor Cells
EthD-1	Ethidium Homodimer-1

ECAR	Extracellular Acidification Rate
FBS	Fetal Bovine Serum
FMO	Flavin Monooxygenases
FMD	Flow-Mediated Dilation
FOXO	Forkhead Box O
F6P	Fructose 6 Phosphate
G6P	Glucose 6 Phosphate
GLUT 1/ SLC2A1	Glucose Transporter 1
Hk2	Hexokinase 2
HAECs	Human Aortic Endothelial Cells
HUVECs	Human Umbilical Vein Endothelial Cells
ICM	Inner Cell Mass
JmjC	Jumonji-C Domain-Containing Proteins
LIF	Leukemia Inhibitory Factor
LT-HSCs	Long-Term Hematopoietic Stem Cells
mTOR	Mechanistic Target of Rapamycin
MSCs	Mesenchymal Stem Cells
mtDNA	Mitochondrial DNA
MitoQ	Mitochondrial-Targeted Coenzyme Q
MEFs	Mouse Embryonic Fibroblasts
mESCs	Mouse Embryonic Stem Cells
NAC	N-Acetylcysteine
NSCs	Neural Stem Cells

NEAA	Nonessential Amino Acids
Oct4	Octamer-Binding Transcription Factor 4
OxPHOS	Oxidative Phosphorylation
OCR	Oxygen Consumption Rate
PFA	Paraformaldehyde
P/S	Penicillin/Streptomycin
PPP	Pentose Phosphate Pathway
PBS	Phosphate Buffered Saline
Psat1	Phosphoserine Aminotransferase 1
PSCs	Pluripotent Stem Cells
POLGA	Polymerase Gamma A
Pkm2	Pyruvate Kinase M2
ROS	Reactive Oxygen Species
RFU	Relative Fluorescent Units
RPM	Revolutions Per Minute
RT	Room Temperature
SAM	S-Adenosyl Methionine
SAMR1	Senescence-Accelerate Mouse Resistant 1
SAMP8	Senescence-Accelerated Prone Mouse Strain 8
Sox2	Sex Determining Regino Y-Box 2
SIRT1	Sirtuin 1
SSEA-1	Stage Specific Embryonic Antigen-1
SE	Standard Error

SOD1	Superoxide Dismutase 1
TET	Ten-Eleven Translocation
TDH	Threonine Dehydrogenase
TCA	Tricarboxylic
TMAO	Trimethylamine N-oxide
H3K4me3	Tri-Methylation of Histone H3 lysine-1
T2DM	Type 2 Diabetes Mellitus
UCP2	Uncoupler Protein 2
VSMCs	Vascular Smooth Muscle Cells
VMCVM	Virginia-Maryland College of Veterinary Medicine
αKG	α-Ketoglutarate

1. CHAPTER ONE: LITERATURE REVIEW

1.1 Abstract

The small metabolite, trimethylamine-N-oxide (TMAO), which is derived from gut microbial metabolism of dietary ingredients such as choline and L-carnitine that are found in foods such as red meat, fish, and eggs has garnered much attention in the past few years from the biomedical community. TMAO is highly associated with a number of chronic disease conditions, including atherosclerosis, stroke, Alzheimer's Disease, diabetes, and chronic kidney disease. A number of studies have been conducted to better understand TMAO's role in these diseases, elucidating several mechanisms of action, including induction of inflammatory pathways and excessive reactive oxygen species (ROS) production, ultimately leading to senescence or apoptosis in several cell types. To date, no one has explored whether TMAO will have an impact on embryonic stem cells. These stem cells, as well as most stem cell types found in the body throughout the human life span, are highly sensitive to ROS, which can serve as a regulator of stem cell potency. In fact, many recent studies have provided substantial evidence to suggest a strong interplay between a stem cell's metabolic state and the maintenance of potency. Stem cells have myriad mechanisms in place to tightly regulate and maintain redox balance in order to prevent the onset of premature differentiation, apoptosis, or senescence. No one yet has drawn a link between the potential harmful effect of TMAO on the body's stem cell populations, and how this may be a contributing factor in TMAO's role in the development of several different chronic diseases. This review provides a strong impetus for the study of TMAO and other metabolites which may increase oxidative stress in stem cells and disrupt the redox balance critical for maintaining their long-term self-renewal and regenerative capacity.

1.2 Introduction

Increasingly, studies have been focusing on the influence of metabolites on the regulation of gene expression and the epigenetic landscape of pluripotent stem cells (PSCs) which in turn can influence the pluripotent state (1). Moreover, it is now clear that cells modulate their metabolic activity depending on the substrates available and the needs of the cell (i.e., whether it is in a state of dormancy, rapid growth, proliferation, or differentiation) (2). This understanding has opened the door to providing new insights into how exogenous metabolites, such as TMAO may impact stem cell potency. TMAO is of particular interest because it is an independent risk factor for several chronic and age-related diseases, and it has been shown to induce inflammation and oxidative stress in a number of cell and tissue types (3-7). In this review, I detail the implication of TMAO in chronic and age-related disease as well as potential underlying mechanisms of action which have been elucidated by several studies. I also review the unique metabolic pathways utilized by pluripotent and adult stem cells and the metabolic changes that take place during differentiation. I discuss all of the recent work which has demonstrated the strong interplay between pathways which regulate metabolism and those that regulate potency, and how oxidative stress is tightly regulated in stem cells in order to maintain the pluripotent state.

1.3. Trimethylamine N-oxide (TMAO)

1.3.1. TMAO and its Biological Roles

TMAO is a small organic compound with the chemical formula $(CH_3)_3NO$ and molecular weight of 75.1 Daltons. It has been studied by marine biologists for a long time, because it is utilized in marine animals to withstand the harsh conditions of the deep ocean, by acting as an osmolyte to counteract the protein de-stabilizing effects of urea and hydrostatic pressure. In fact,

it has been shown in several different marine animal species that TMAO concentration increases linearly with depth up to 4.8km (8). How TMAO promotes protein stabilization is a subject of debate, but several studies suggest that TMAO increases the hydrogen bonds of water molecules, which enhances water structure. As a result, the peptide bonds of proteins are less likely to interact with the water molecules and become disrupted, thereby preventing protein unfolding (9, 10).

TMAO is widely consumed by humans, especially in western cultures where red meat and egg consumption are high. TMAO is found in fish in its preformed state, and it can also be converted from trimethylamine (TMA), which is generated through gut microbial metabolism of dietary choline, phosphatidylcholine (lecithin), and L-carnitine. TMA is oxidized to TMAO by hepatic flavin monooxygenases (FMO's), primarily FMO3. TMAO then circulates the plasma where it can accumulate in the tissues and is eventually cleared by the kidney. Red meat, eggs, dairy products and salt-water fish are all sources of TMAO as they contain choline, lecithin, and carnitine (11). Several studies have demonstrated that the production of TMAO is dependent on metabolism by intestinal microbiota. In gnotobiotic mice colonized with TMAO-producing bacteria, TMAO accumulated in the serum; while no TMAO accumulated in the serum of mice colonized with non-TMAO-producing bacteria (12). Studies in humans given phosphatidylcholine challenge (13) or L-carnitine challenge (4) found that TMAO plasma levels were suppressed by oral administration of broad spectrum antibiotics. One study did, however, suggest that TMAO consumed in its preformed state, such as in fish, may be absorbed independent of gut microbes, since circulating TMAO concentrations were increased within 15 minutes after fish consumption, a time frame too short for microbial and hepatic processing (14).

Plasma TMAO levels vary widely between individuals, and are influenced by a host of variables, including diet, gut microbial flora, age, liver FMO enzymes, and renal function. A genome-wide association study with 1973 human subjects, determined that genes have little influence over TMAO levels (15). Koeth et al., found that a person's long-term dietary habits largely impacted plasma TMAO concentration during L-carnitine challenge. Vegan participants produced significantly less TMAO at baseline with little increase after L-carnitine challenge, whereas participants that regularly consumed meat had significantly higher plasma TMAO levels and a much higher spike after the L-carnitine challenge. The enterotype was also found to be different for the two groups with enriched proportions of the genus *Prevotella* associated with higher circulating plasma TMAO, compared to the enterotype enriched in *Bacteroides*. This indicates that an individual's dietary habits largely determine the composition of the intestinal microbiota and thus its ability to generate TMAO (4). Additionally, fasting plasma TMAO levels in healthy subjects was shown to increase significantly with age in humans and mice (3, 6, 16). Higher FMO3 expression results in higher TMAO production. In female mice, FMO3 expression is 1,000 fold higher than that in male mice, resulting in higher plasma TMAO levels and more severe atherosclerotic plaque development than in male mice, even when fed the same diet. This gender difference in FMO3 expression is not seen in humans, and consequently studies have shown no significant gender difference between plasma TMAO levels in humans (5, 16). TMAO must be excreted through urine, so impaired renal function leads to increased serum levels of TMAO, which can be decreased substantially following kidney transplantation (17, 18).

1.3.2. Implication of TMAO in Chronic and Age-Related Diseases

TMAO did not enter the limelight in the biomedical research field until recently when several studies associated high plasma TMAO levels with an increased risk for a host of chronic

diseases, including cardiovascular disease, chronic kidney disease (CKD), diabetes, and neurodegenerative disorders. Using a metabolomics approach, Wang et al. discovered for the first time that a cluster of three phospholipid-associated molecules choline, betaine, and TMAO, was associated with atherosclerosis (5). Since then, numerous recent case–control and longitudinal studies have confirmed a strong association between plasma TMAO levels and risk of atherosclerosis in several different cohorts (4, 13, 19). The association between high TMAO and cardiovascular events is significantly increased in patients with type 2 diabetes mellitus (T2DM), and high circulating TMAO levels were independently associated with T2DM in humans and mice (20, 21). In addition, TMAO can be detected in human cerebral spinal fluid and clinical data has revealed that increased TMAO plasma levels are associated with increased risk of cerebrovascular disease, stroke, and Alzheimer's Disease (AD) (7, 22-24). As mentioned earlier, TMAO must be cleared by the kidney, therefore, impairment of kidney function results in increased plasma TMAO levels (25, 26). Interestingly, elevated TMAO is also a biomarker for renal disease, which provides an indication as to why patients with CKD are often also at higher risk for developing cardiovascular disease (CVD) (17, 27).

1.3.3. Current Understanding of Underlying Mechanisms for TMAO-Induced Cellular Abnormalities

A multitude of in vivo and in vitro studies have been conducted to investigate the potential mechanism underlying how TMAO promotes the onset of several chronic diseases. The main mechanisms of action of TMAO appear to be through inducing vascular inflammation, oxidative stress, and senescence.

TMAO first emerged in the biomedical field as an independent risk factor for atherosclerosis, and therefore, the underlying mechanism for its role in this disease has been the

most well-studied to date. TMAO's role in promoting atherosclerosis has been elucidated from studies conducted both in vivo with apoe-/- and LDLR-/- mice, murine models for atherosclerosis, and in vitro with endothelial cells, vascular smooth muscle cells, monocytes, macrophage cells, and endothelial progenitor cells. Several studies demonstrated that TMAO enhanced atherosclerotic plaques in atherosclerosis-prone mouse models (4, 5, 28, 29). In these models, TMAO increased macrophage cholesterol accumulation and foam cell formation through enhanced levels of macrophage scavenger receptors, CD36 and SRA-1, and reduced reverse cholesterol transport (4, 5, 28). Additionally, chronic choline exposure resulted in vascular inflammation in atherosclerosis-prone mice through enhanced expression of proinflammatory cytokines, such as TNF-α, ICAM1, and VCAM1 (7, 28). Activation of inflammatory signaling was also seen after acute TMAO exposure in vivo, with increased abundance of total p65 NF-kB in the mouse aortas and elevated expression of inflammatory genes (7). In vitro studies conducted with human aortic endothelial cells (HAECs) and vascular smooth muscle cells (VSMCs) also showed upregulation of inflammatory markers and enhanced leukocyte adhesion, effects which were abolished with treatment of NF-kB inhibitors (7, 30). Sun et al. found that TMAO significantly stimulated oxidative stress and the expression of TXNIP-NLRP3 inflammasome, resulting in the dose- and time-dependent release of inflammatory cytokines interleukin (IL)-1β and IL-18 and decrease in endothelial nitric oxide synthase (eNOS) in human umbilical vein endothelial cells (HUVECs), results which were reversed with NAC antioxidant treatment. Ke et al. demonstrated that TMAO inhibits SIRT1 expression, induces oxidative stress, impairs NO production, and enhances the expression of endothelial cell senescence markers in vivo and in vitro (3). ROS-induced endothelial dysfunction was also seen in endothelial progenitor cells (EPCs). In humans with stable angina,

plasma TMAO levels were negatively correlated with circulating EPC numbers and flow-mediated dilation (FMD). In vitro studies with human EPCs found that TMAO induced cellular inflammation (e.g., upregulation of IL-6, CRP, and TNF-α), oxidative stress, and downregulation of NO production, ultimately suppressing EPC functions (31). These results help to explain why TMAO accelerates endothelial dysfunction, foam cell formation, and monocyte adhesion in the progression of atherosclerosis.

To investigate the role of TMAO in cognitive impairment and neurodegenerative disorders, Li et al., compared the impact of TMAO in senescence-accelerated prone mouse strain 8 (SAMP8) and senescence-accelerate mouse resistant 1 (SAMR1) mice. TMAO was found to down-regulate mTOR signaling, resulting in reduced expression of synaptic plasticity-related proteins. It also led to mitochondrial dysfunction, increased ROS production, and a higher number of senescent cells in the hippocampal CA3 region. Altogether, TMAO exposure induced brain aging and age-related dysfunction in SAMR1 mice and aggravated the cerebral aging process of SAMP8 mice (6). These results help to explain TMAO's association with cerebrovascular disease, stroke, and AD (7, 22, 23). TMAO appears to induce ROS production and senescence in several cell types, which may point to its role in the aging process and its implication in many chronic diseases.

1.4. Mouse Embryonic Stem Cells

1.4.1. Source, Role, and Basic Characteristics

Mouse embryonic stem cells are derived from the developing embryo and can be categorized into two groups – naïve and primed states, which correspond to the pre-implantation stage of embryonic development, and the early post-implantation stage, respectively (32, 33).

These two groups of cells are derived from different stages of embryonic development and exhibit significant differences, including gene expression, epigenetic modifications, metabolism, and differentiation ability (34). This project works with naïve embryonic stem cells, which means they are derived from the inner cell mass (ICM) of the pre-implantation blastocyst. These cells are pluripotent stem cells, and they are characterized by their ability to give rise to cells of all three germ layers (i.e., endoderm, ectoderm, and mesoderm), colonize mouse embryos, and proliferate indefinitely in vitro. Pluripotent cells are defined by a group of transcription factors, including Oct4, Sox2, and Nanog, among others. Embryonic stem cells represent a critical stage in the first few days of embryonic development when the cells are still in a pluripotent state and primarily utilize aerobic glycolysis. These cells are able to maintain a lower mutational rate compared to differentiated cells due to an enhanced antioxidant system, effective DNA repair, and low levels of oxidative stress. Changes in mESC genome could lead to serious consequences, such as fetal lethality or congenital disease. Moreover, mESCs with accumulated mutations undergo apoptosis or differentiation to preserve the population genome (35-37).

1.4.2. In Vivo Environment

mESCs reside within the inner cell mass of the blastocyst, which is formed and released into the uterine cavity around Gestational Days 3-4 in mice (38). Once inside the uterine cavity, the blastocyst is able to receive nutrients via endometrial secretions. These secretions have been shown to contain a complex array of lipids, proteins, and carbohydrates (39). In addition to the ICM, the blastocyst contains a layer of cells called the trophoblast which contains cells that will later go on to form the placenta. The entire blastocyst is surrounded by an outer protective coat called the zona pellucida, which is an extracellular matrix made up of glycoprotein filaments (38). Once the blastocyst has fully formed, it will undergo “hatching” where it sheds the zona

pellucida, exposing the blastocyst to the uterine epithelium. Soon, cytoplasmic projections can be seen protruding from the trophoblast in order to invade the maternal tissue. The trophoblast contains enzymes that will digest the maternal tissue in order to initiate blastocyst implantation (40). Eventually, the trophoblast will establish contact between the maternal blood supply and the ICM of the blastocyst (41, 42). Following implantation, the embryonic stem cells lose their pluripotency as the cells differentiate to form the three germ layers in the process of gastrulation. This will trigger significant metabolic remodeling in the implanted blastocyst and the pluripotent cells within it, allowing the cells to differentiate and commit to different cell fates. If embryonic stem cell properties are impaired during this time, then most likely the blastocyst will be unable to implant into the uterine lining, resulting in loss of the embryo (43).

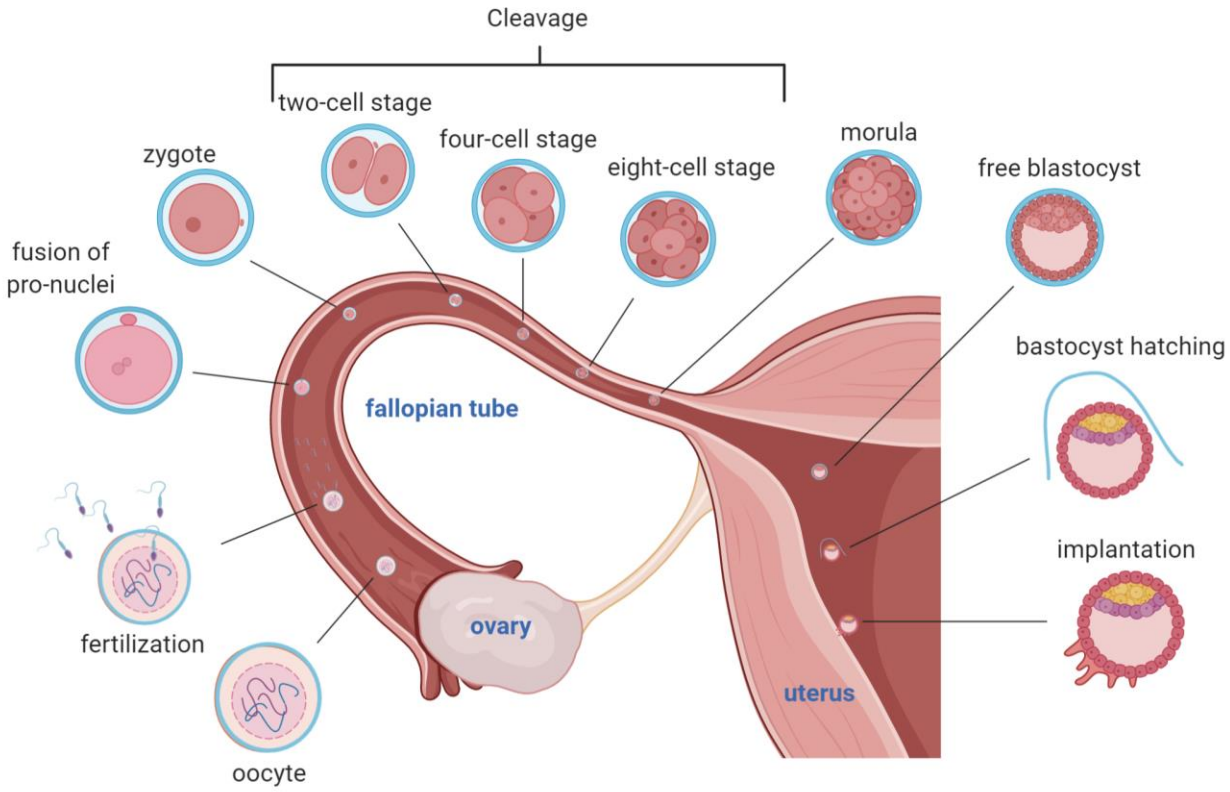

Figure 1.1 In vivo environment of embryonic stem cells. Early embryonic development consists of zygote formation, followed by cell cleavage, and formation of the early blastocyst. The cells of the blastocyst segregate into the trophectoderm and inner cell mass (ICM), which contains the embryonic stem cells (ESCs). The blastocyst sheds its outer protective layer, the zona pellucida, in a process called "hatching". Then, enzymes of the trophectoderm facilitate blastocyst implantation. Created with BioRender.com.

1.4.3. Overview of Potent Cell Types

Throughout the different stages of embryonic development and the entire life span of an organism, stem cells of different levels of potency (i.e., differentiation ability) are present. The first type of stem cell that arises in embryonic development occurs when the ovum and sperm

fuse to form a totipotent stem cell. Totipotent stem cells have the highest level of potency as they are capable of forming all cell types (i.e., cells of both embryonic and extraembryonic tissue) and of generating a globally coordinated developmental sequence in order to form a complete organism. Totipotent stem cells are present from the time of zygote formation until the early-cleavage blastomere. Next, are plenipotent stem cells, which have the same differentiation ability of the totipotent cell, but are not capable of coordinating the entire process of development. Once the blastocyst matures enough to segregate into the ICM and trophoblast, pluripotent stem cells (PSCs) can be found within the ICM, and are capable of forming cells of all three germ layers (44). Once the blastocyst implants, PSCs begin to differentiate and commit to different cell fates. This will result in the generation of multipotent and progenitor stem cells for different tissue types that will contribute to the process of embryonic and fetal development into the final offspring. In addition, some stem cells and progenitor cells will remain in these tissues for the rest of the human life span, termed somatic or adult stem cells. These stem cells have a relatively restricted ability to self-renew and differentiate; however, they play a critical role in the maintenance of adult tissues, and in some cases can activate to repair and/or regenerate damaged tissues (45, 46). The loss of potency is a gradual process, and how these cells acquire a different transcriptional state as they commit to different cell fates remains largely unknown. What researchers have observed, however, is that metabolism promotes cell fate regulators and stage-specific regulators also modulate metabolism (1, 2). Therefore, understanding the impact of exogenous metabolites on stem cell metabolism may reveal mechanisms for diseases related to loss of potency. Several papers have identified direct links between mitochondrial metabolism and the regulation of pluripotency pathways as will be discussed below.

1.5. Stem Cell Metabolism

1.5.1. Overview of Metabolic Pathways

Glycolysis is one of the major energy-producing pathways in living cells, and it utilizes carbohydrates to generate ATP, NADH and pyruvate. When oxygen is present, pyruvate is transported to the mitochondrial matrix and converted into acetyl-CoA. In addition, many cells utilize other metabolic pathways, such as β-oxidation, which forms acetyl-CoA from the breakdown of fatty acids. Acetyl-CoA formed from either glycolysis or β-oxidation, then enters the tricarboxylic (TCA) cycle where it gets further oxidized, generating the electron carriers, NADH and FADH2. These electron carriers transport their electrons to the electron transport chain (ETC), which is made up of protein complexes that will harness the energy from electrons as they are being transferred across the chain in order to pump protons into the mitochondrial inner membrane space, which will generate an electrochemical gradient that stimulates ATP production through ATP synthase. This process in which oxygen consumption is coupled with ATP production, is called oxidative phosphorylation (OxPHOS), and produces most of cellular ATP. Cells will utilize different metabolic pathways based on their needs and the substrates available in their microenvironment (1). For example, cardiomyocytes require high amounts of energy and are non-proliferative, so they rely mostly on β-oxidation, which generates the highest net ATP production (47). On the other hand, highly proliferative cells will prioritize the generation of biomass through glycolysis, even though it results in less efficient ATP production (48).

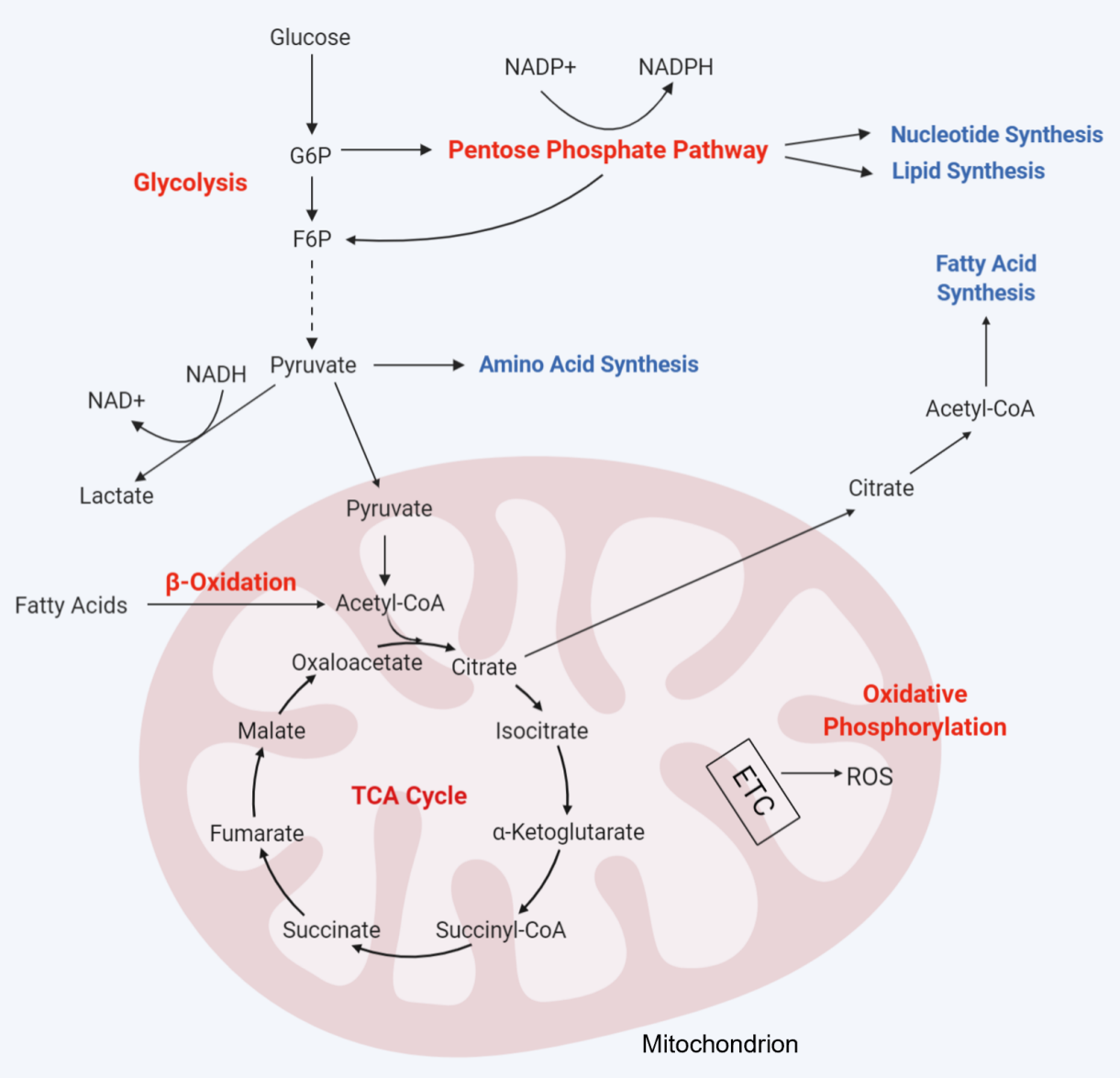

Figure 1.2 Overview of metabolic pathways. The major metabolic pathways are highlighted in red and include glycolysis, pentose phosphate pathway (PPP), oxidative phosphorylation, β-oxidation, and tricarboxylic (TCA) cycle. CoA, coenzyme A; ETC, electron transport chain; F6P, fructose 6 phosphate; G6P, glucose 6 phosphate; ROS, reactive oxygen species. Created with BioRender.com.

1.5.2. Metabolic Activity of Pluripotent Stem Cells

The dramatic changes that take place in the physiology of the embryo during the first steps of mouse gestation described above appear to be facilitated by changes in metabolic activity. Embryonic stem cells have unique metabolic requirements based on the function they play in the pre-implantation blastocyst. Since the pluripotent cells of the ICM must give rise to all of the cells and tissues of the final offspring, these cells are designed to minimize ROS production and avoid DNA damage. In addition, the rapid proliferation rate of these cells requires energy, but mostly it requires the synthesis of building blocks to assemble new daughter cells. These metabolic requirements are reflected in their mitochondrial morphology, utilization of glycolysis and anabolic pathways, and enhanced antioxidant system. During formation of the blastocyst, mitochondrial numbers are halved with each cell division. As a result, these cells have relatively few mitochondria, with mostly perinuclear localization and immature cristae (49-51). Therefore, although these cells have active mitochondria, their respiratory capacity and overall rate of oxygen consumption is lower than their differentiated counterparts. ESCs mostly utilize aerobic glycolysis for ATP production as is evident by high glucose uptake and lactate production (52). The main advantages of utilizing glycolysis over OxPHOS are to reduce ROS generation in the mitochondrial respiratory chain and to generate the intermediary metabolites required for anabolic pathways. The pentose phosphate pathway (PPP) is highly active in mESCs and maintained by high glycolytic flux. The PPP shunts glucose-6-phosphate from glycolysis in order to generate precursors for fatty acid synthesis, nucleotide synthesis, and can re-enter glycolysis in order to generate ATP. Specifically, it generates 5-phosphoribosyl-1-pyrophosphate (PRPP) for pyrimidine and purine synthesis. Additionally, it generates NADPH, which is utilized for fatty acid synthesis and to generate reduced glutathione, an antioxidant that reduces H_2O_2 to

H_2O and ultimately lower oxidative stress. Moreover, ablation of glucose-6-phsophate dehydrogenase, the rate-limiting step in the PPP, results in elevated sensitivity of mESCs to oxidative stress, and causes them to undergo apoptosis, while their wild type counterparts are able to tolerate the same ROS concentrations (53). As a result, regardless of oxygen availability, ESCs will utilize aerobic glycolysis to meet their energy needs, instead of pyruvate oxidation in the mitochondria. This strategy is also observed in highly proliferative cancer cells and is termed the Warburg Effect (48). Interestingly, although PSCs mainly utilize glycolysis, these cells still rely on the TCA cycle to generate intermediates for anaplerotic pathways and maintenance of the epigenome. Moreover, blocking acetyl-CoA production has been shown to cause loss of pluripotency, because it prevents histone modifications which are critical for maintenance of the pluripotent state (54, 55). The metabolic switch that takes place during the onset of differentiation is accompanied by full oxidation of pyruvate in the mitochondria, resulting in acetyl-CoA consumption, loss of histone modification, and subsequent loss of the pluripotent state (54).

1.5.3. Metabolic Activity of Differentiating Cells

Differentiation is a gradual process, and it requires a metabolic switch from glycolysis to OxPHOS. The transition that occurs in metabolic pathways at the time of implantation is critical for the developing embryo, as disruption of metabolic features reduces implantation capacity and embryonic viability. This metabolic switch is accompanied by changes in mitochondrial morphology and localization as the mitochondria become more elongated, with more developed cristae and cytoplasmic distribution (49, 50). Additionally, there is rapid mitochondrial DNA (mtDNA) replication and a large uptake in oxygen consumption as ETC coupling with ATP production increases. During differentiation, there is a repression of key enzymes involved in the

PPP and lipid biosynthesis pathways (50). Further, treatment with glycolysis inhibitors, 2-deoxyglucose (2-DG) or 3-bromopyruvate (3-BrPa), can stimulate this loss of pluripotency (54). As a result, there is a sharp decrease in glycolytic flux and lactate production upon mESC differentiation. The mitochondria are more mature, with greater respiratory reserve capacity, and therefore, can perform OxPHOS more efficiently. This allows for pyruvate to become fully oxidized and be able to fully couple glycolysis to the TCA cycle. Additionally, ETC activity increases and is able to efficiently couple oxygen consumption to ATP production. This results in greater ROS production, which further promotes the process of differentiation (2).

1.5.4. Metabolic Activity of Quiescent Adult Stem Cells and Progenitor Stem Cells

Most adult stem cells, including long-term hematopoietic stem cells (LT-HSCs), mesenchymal stem cells (MSCs) in the bone marrow, and neural stem cells (NSCs) in the brain are quiescent. Quiescent adult stem cells likely lie dormant and maintain a slow-cycling state in order to minimize ROS-induced cellular damage and ensure life-long tissue renewal capacity (2, 56). LT-HSCs, MSCs, and NSCs have all been shown to be sensitive to ROS, and under conditions of oxidative stress enter differentiation, senescence, or apoptosis (57-59). As a result, these cells share similar metabolic activity to PSCs in that they utilize glycolysis to a greater extent, have lower mitochondrial mass, and relatively low rates of OxPHOS (60, 61). Similar to PSCs, differentiation of these adult stem cells will trigger an increase in mtDNA replication and the rate of OxPHOS. Interestingly, these adult stem cells share several nutrient-sensitive signaling pathways that regulate the balance between quiescence and proliferation. For example, forkhead box O (FOXO) family of transcription factors has a key role in the oxidative stress response in LT-HSCs and NSCs (57, 58). During the process of differentiation, FOXO becomes

rapidly degraded, allowing ROS levels to increase and further promote differentiation, a mechanism also observed in mESCs.

1.5.5. Pluripotent Stem Cells as a Model for Other Potent Cells

Typically, pluripotent stem cells are viewed as a model for cells of the ICM in the pre-implantation embryo; however, as alluded to above, these cells also serve as a model for other potent cells in the body. Several studies have demonstrated that mitochondria act as regulators of potency in all types of stem cells. The mitochondrial bioenergetics of the cell play an important role in the cell's ability to adapt to its environment and prevent damage under oxidative stress. Interestingly, PSCs and adult tissue stem cells share many of the same metabolic pathways during the maintenance and loss of pluripotency. Recent studies have demonstrated that the loss or acquisition of potency, whether it is in PSCs or quiescent adult stem cells, is facilitated by a metabolic switch (55). The metabolic pathways utilized by ESCs and other stem cell types share a heavy reliance on glycolysis that switches to OxPHOS during differentiation. Further, both ESCs and adult tissue stem cells are highly sensitive to factors such as increased oxidative stress and inflammation, which have been shown to alter the tightly regulated metabolic pathways of these cells, resulting in premature differentiation, senescence, or apoptosis (36, 57-59). Therefore, the study of how TMAO impacts mESC potency can provide an indication of how TMAO may impact other stem cell types that are present into adulthood.

1.6. Cellular Metabolism Dictates Stem Cell Potency

1.6.1. Molecular Metabolic Pathways Implicated in Maintaining Pluripotency

Traditionally, cellular metabolism has been studied for its crucial role in generating energy for the cell; however, more recently metabolism has been implicated in stem cell activity

and cell-fate determination (1, 2). Several studies have uncovered some of the molecular metabolic pathways unique to PSCs. Mostly, these mechanisms are in place to promote glycolytic flux and anabolic pathways, so that the cell can generate enough energy and building blocks to fuel its rapid proliferation and maintain pluripotency (54, 55). Because aerobic glycolysis is central to the metabolic needs of PSCs, it's logical that the pathways which regulate pluripotency and metabolism are interconnected.

Recent studies have demonstrated that the core pluripotency factors (i.e., Oct4, Sox2, Nanog) can directly regulate glycolysis through inducing expression of glucose transporters and key glycolytic enzymes. Glucose transporter 1 (GLUT 1/SLC2A1) is highly expressed in PSCs and required for their survival through the maintenance of high glycolytic flux (55, 62). Yu et al., demonstrated that the core transcriptional factors, sex determining region Y-box 2 (Sox2), octamer-binding transcription factor 4 (Oct4), and Nanog can directly bind to the GLUT1 enhancer to induce GLUT1 expression in order to increase glucose uptake and promote glycolysis (63). Additionally, Oct4 has been shown to maintain high glycolytic flux by directly regulating the key glycolytic enzymes, hexokinase 2 (Hk2) and pyruvate kinase M2 (Pkm2). Furthermore, overexpression of these glycolytic enzymes retained pluripotency in the absence of leukemia inhibitory factor (LIF), which is the growth factor required in mESC culture to maintain mESC properties (64). The transcription factor and key regulator of pluripotency, c-Myc, has also been shown to promote glycolysis. Mbd2 acts as a transcriptional repressor of glycolysis by directly binding to the Myc promoter to repress Myc expression (65). Cao et al., identified a cluster of miRNAs (miR-290 cluster) which represses Mbd2, and in turn increases the expression of Myc and its downstream transcriptional targets, PKM2 and lactate dehydrogenase A (LDHA), both of which are glycolytic enzymes (65). These studies

demonstrate the coordination and interdependence between the pathways that regulate pluripotency and those that regulate metabolism.

1.6.2. Role of Metabolites on Epigenetics and Stem Cell Fate

Metabolism can act as a driver of stem cell fate through its influence on the epigenome and gene expression. ESCs must maintain a unique open chromatin structure in order to maintain a pluripotent state that is highly plastic and poised for differentiation. Key metabolites from intracellular and exogenous sources can significantly influence histone and/or DNA epigenetic modifications, thereby providing a link between metabolism and maintenance of the pluripotent state. In general, tri-methylation of the Lys 4 residue of histone H3 (H3K4me3) and H3 acetylation are associated with a transcriptionally active state, whereas H3K9me3, H3K27me3, and DNA methylation function as repressive chromatin marks (66, 67). ESCs require a delicate balance of chromatin modifications, in which low levels of chromatin repressive marks are required for repression of lineage specific genes to prevent the onset of differentiation. Wang et al., identified threonine as the only amino acid critically required for mESC growth and pluripotency. Threonine is utilized in one-carbon metabolism by the folate pool, which is especially important for mESCs, because it generates metabolites for anabolic pathways and epigenetic modifications. In threonine catabolism, the rate-limiting step is oxidation by the enzyme threonine dehydrogenase (TDH), which converts threonine to glycine and acetyl-CoA. Expression of TDH in PSCs is extremely high compared to differentiated cells, which may explain why PSCs also have higher amounts of acetyl-CoA compared to differentiated cells (54, 68). When TDH expression was repressed, it resulted in reduced expression of pluripotency markers (*Oct4*, *Sox2*, *Nanog*), and an increased expression of differentiation markers (*Foxa2* and *Sox17*). Metabolism of threonine and S-adenosyl methionine (SAM) are coupled. SAM is an

important methyl donor responsible for H3K4me3 and highly expressed in PSCs. This epigenetic modification is important for maintaining euchromatin, which is crucial for epigenetic plasticity in mESCs. Additionally, Shyh-Chang et al., found that several Thr-SAM pathway inputs such as Thr, Cys, and folate were less abundant in mESCs than in mouse embryonic fibroblasts (MEFs), while downstream outputs, such as SAM and cystathionine were more abundant (69). These studies demonstrate how the Thr-SAM pathway provides a strong link between metabolism and epigenetic regulation of the pluripotent state.

Histone acetylation also plays a key role in the maintenance of the open chromatin structure of PSCs. Moussaieff et al., demonstrated that glycolytic production of acetyl (Ac)-CoA, provides an important substrate of histone acetylation. Instead of completing the TCA cycle, pyruvate is incompletely oxidized to citrate, which is transported to the cytoplasm to produce Ac-CoA through the enzyme ATP-citrate lyase (ACL), for H3K9/K27 acetylation (54, 70). Just 24 hours after spontaneous differentiation, a metabolic switch occurs in which pyruvate undergoes full oxidation in the TCA cycle, resulting in loss of H3K9/K27 acetylation and the pluripotent state (54). This supports the notion that PSCs require the TCA cycle for anaplerotic pathways in order to maintain the epigenome, and the decision of whether to fully oxidize pyruvate in the mitochondria is tightly regulated.

The intermediary metabolite, α-ketoglutarate (αKG), is also generated in mESCs through an incomplete TCA cycle as well as from the catabolism of glutamine. αKG functions as a cofactor for several chromatin-modifying enzymes, such as Jumonji-C (JmjC) domain-containing histone demethylases and the ten-eleven translocation (TET)-family enzymes involved in DNA demethylation (71, 72). Carey et al., demonstrated the importance of an elevated αKG/succinate ratio in promoting histone/DNA demethylation and repressing

differentiation. Specifically, αKG is required for the depletion of repressive chromatin marks, H3K27me3 and H3K9me3, as well as for the reduction of total DNA methylation. The study showed that supplementation with αKG promotes ESC self-renewal, while supplementation with succinate promotes differentiation (73). Loh et al., demonstrated that Jmjd1a and Jmjd2c are direct targets of Oct4, and that the depletion of these histone demethylases results in differentiation. Additionally, the study found that Jmjd2c positively regulates *Nanog* by preventing H3K9me3 and the binding of the corepressor HP1/KAP1 complex at the Nanog promoter (72). Further, it was recently demonstrated that intracellular αKG levels are controlled by phosphoserine aminotransferase 1 (*Psat1)*, which is a direct target of Oct4 (74). Therefore, these pathways provide a direct link between metabolite levels and epigenetic gene regulation in the maintenance of pluripotency.

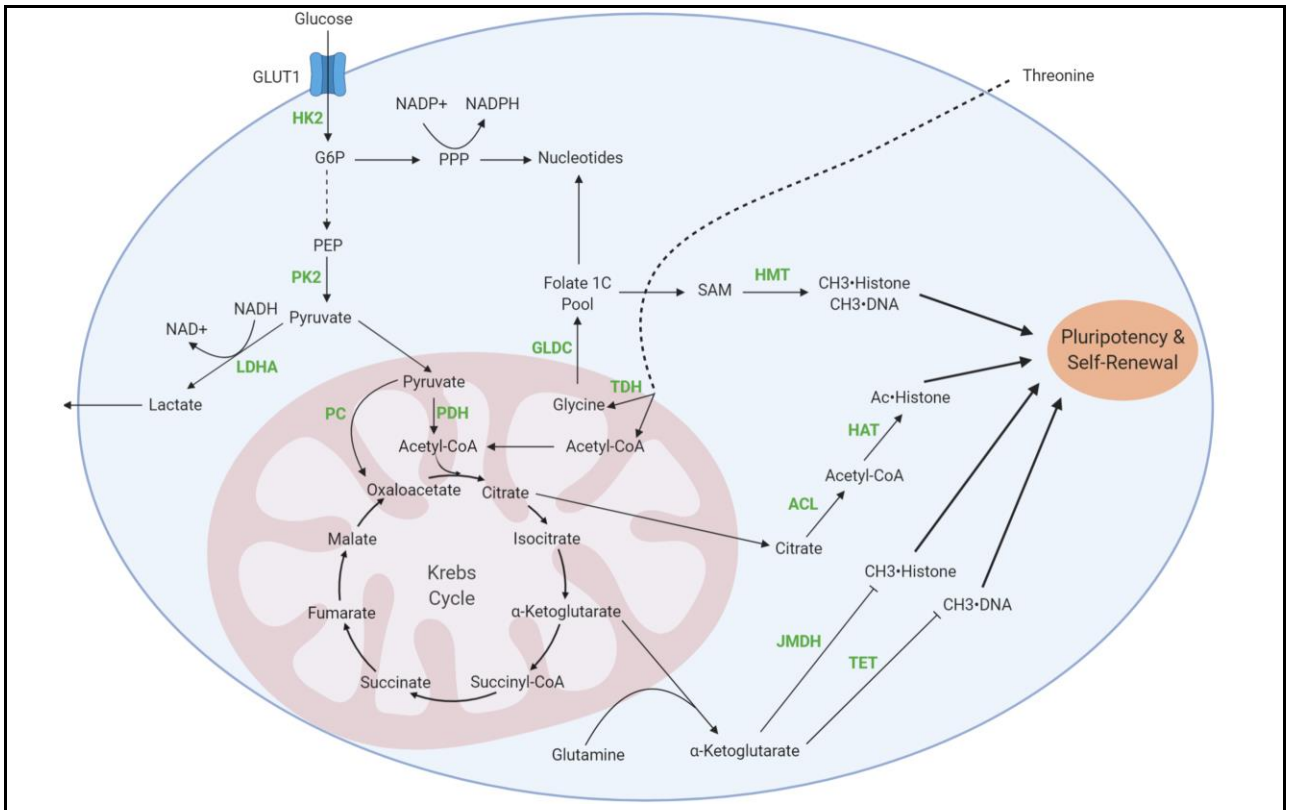

Figure 1.3 Influence of metabolites on the epigenetic landscape and stem cell fate. Metabolism of threonine is coupled with S-adenosyl-L-homocysteine (SAM), which is responsible for histone methylations that maintain the pluripotent state. Pyruvate is incompletely oxidized to citrate for histone acetylation. α-ketoglutarate is generated from the tricarboxylic acid (TCA) cycle and from glutamine catabolism and acts as a cofactor for Jumonji-family histone demethylases (JMDHs) and the Tet methylcytosine dioxygenase (TET)-family enzymes involved in DNA demethylation. Ac, acetylation; ACL, ATP-citrate lyase; CH3, methylation; CoA, coenzyme A; GLDC, glycine decarboxylase; G6P, glucose-6-phosphate; HAT, histone acetyltransferase; HK2, hexokinase 2; HMT, histone methyltransferase; PC, pyruvate carboxylase; PDH, pyruvate dehydrogenase complex; PEP, phosphoenolpyruvic acid; PK2, pyruvate kinase 2; PPP, pentose phosphate pathway; TDH, threonine dehydrogenase; TET, Ten-Eleven Translocation. Created with BioRender.com.

1.7. Oxidative Stress Induces Metabolic Switch and Loss of Potency in PSCs

1.7.1. Major Sources of Intracellular ROS

ROS include a wide array of molecules which are free radicals that contain oxygen and are typically highly reactive. Although ROS may be generated in various parts of the cell, the major source of ROS is in the mitochondrial ETC. In the ETC, electrons are transferred from complex I to complex IV where oxygen is the final electron acceptor. Additionally, oxygen molecules may prematurely accept electrons that leak from complexes I and III (75). Once oxygen accepts an electron, it leads to a cascade of reactions which generate different types of oxygen radicals, some of which can react with almost any other molecule in the cell. Oxygen accepts the electron and forms superoxide anion (O_2^-•), which is converted to H_2O_2 by SOD. H_2O_2 is then converted to H_2O by catalase, or may react with a metal such as Fe^{2+} to produce a hydroxyl radical (OH•), which is extremely reactive (76). The formation of these highly reactive oxygen molecules is problematic because their unpaired electrons may react with and cause damage to cellular structures, including proteins, lipids, and DNA. DNA oxidation is of particular concern because it damages the DNA and increases the likelihood of DNA mutations (77). Cells have limited capacity for the repair of oxidized proteins, so it usually results in their ubiquitination and degradation by the proteasome. Protein oxidation may also promote the formation of insoluble protein aggregates, which is the molecular basis for many diseases (76, 78). Therefore, excessive ROS generation is detrimental to cell viability, and is especially important in mESCs where ROS plays a role in directing cell fate. As a result, mESCs have evolved complex mechanisms for maintaining redox balance: (1) they minimize ROS production by mostly utilizing glycolysis for ATP instead of OxPHOS; (2) they have a highly active PPP

which generates intermediates required to neutralize ROS; and, (3) they utilize uncoupler proteins to lower the mitochondrial membrane potential in order to lower oxidative stress.

1.7.2. Impact of ROS on Stem Cell Viability and Potency

Several recent papers have identified key pluripotency and apoptotic pathways that are activated by ROS in ESCs. Excessive ROS generation in mESCs activates p53, which directly binds and suppresses *Nanog* expression (79-81). p53 plays an important role in maintaining ESC genomic integrity, which differs from its role in terminally differentiated cells. In somatic cells, p53 induces cell cycle arrest at the G_1/S checkpoint in order to allow for repair of DNA damage; however, mESCs lack a p53-dependent G_1/S checkpoint (82). Instead, in mESCs p53 is mainly cytoplasmic and induces apoptosis in cells with relatively large amounts of DNA damage and induces differentiation in mESCs with minimal DNA damage to allow them to undergo p53-dependent cell cycle arrest or apoptosis after differentiation (36). Excessive ROS generation will result in DNA damage which activates p53-suppression of Nanog gene expression, thereby triggering cell differentiation. As a defense mechanism, simultaneously sirtuin 1 (SIRT1), a p53 deacetylase, is activated in order to inhibit p53 suppression of Nano gene expression (83, 84). SIRT1 also upregulates cellular antioxidant enzymes, including superoxide dismutase 1 (SOD1), catalase, glutathione peroxidase 1, and thioredoxin-1 in order to control ROS levels (85). This mechanism is effective under relatively high levels of ROS; however, when ROS levels continue to rise and overwhelm the cell's antioxidant system, SIRT1 has been shown to mediate mitochondrial-dependent apoptosis through mitochondrial translocation of p53 (79). Upon the onset of mESC differentiation, ROS levels are increased, p53 rapidly downregulates *Nanog*, and expression of SIRT1 and SOD1 are also suppressed (86, 87).

Another important transcription factor in mESC viability and potency is FOXO1, because it controls the expression of Bim and Puma, which are potent proapoptotic proteins. FOXO1 is positively regulated by JNK and negatively regulated by Akt. When ROS levels are too high, it activates JNK, which mediates the activation and nuclear import of FOXO1 to trigger expression of apoptotic genes (84). Akt activation inhibits FOXO1 and promotes longevity in PSCs. However, under conditions of high ROS, SIRT1 can deacetylate FOXO1, which in turn increases FOXO1 DNA binding, and inhibits negative phosphorylation by Akt. Additionally, FOXO1 is believed to directly regulate pluripotent gene expression by binding to sequences within regulatory regions of *OCT4* and *SOX2*. The knockdown of *FOXO1* in hESCs and mESCs leads to loss of pluripotency, indicating that it is an essential component of the pluripotent cell circuitry (88).

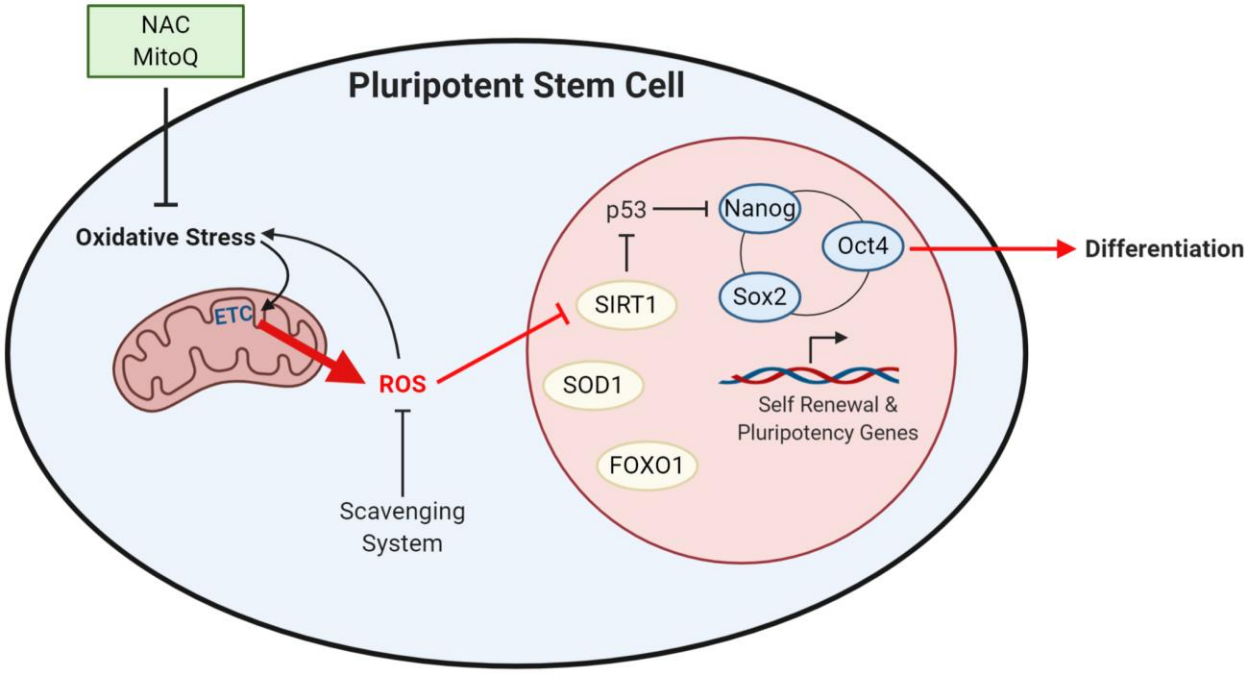

Figure 1.4 ROS acts as a key regulator of pluripotency. Oxidative stress induces excessive mitochondrial ROS generation. Sirt1 inhibits p53 suppression of Nanog expression in order to maintain the pluripotent state; however, excessive ROS generation upsets the balance of these pluripotency pathways, triggering the onset of differentiation, which further promotes ROS production and loss of pluripotency. These ROS-induced negative effects can be rescued with treatment of antioxidants, N-acetyl-L-cysteine (NAC) and mitochondria-targeted ubiquinone (MitoQ) (86). Created with Biorender.com.

1.7.3. Cellular Mechanisms for Controlling Intracellular ROS Levels

One of the main advantages mESCs have for relying mostly on glycolysis rather than OxPHOS is the minimization of ROS production from the ETC. In addition, the PPP is highly active in PSCs and serves as the main source of NADPH, which is the reducing agent utilized by

cytosolic glutathione reductase for the degradation of H_2O_2 (76). Therefore, the metabolic phenotype alone is one way in which stem cells control intracellular ROS levels.

Additionally, several studies suggest that uncoupler protein 2 (UCP2) is upregulated in PSCs, which is critical for maintenance of the pluripotent state (50, 89). It appears to play a pivotal role in controlling ROS levels by influencing the fate of pyruvate and inducing proton leak. The fate of pyruvate plays an important role in maintaining pluripotency. Pyruvate can be utilized in several different metabolic pathways, including: (1) conversion to lactate to recycle NAD+ back into glycolysis; (2) conversion to acetyl-CoA for entry into the TCA cycle; and (3) conversion to oxaloacetate to enter the TCA cycle and generate metabolic intermediates for anabolic pathways. In PSCs, pyruvate is mainly converted to lactate, and the remaining pyruvate is used in anaplerotic pathways to replenish TCA cycle intermediates. Zhang et al found that UCP2 is highly expressed in PSCs and functions to impair glucose oxidation, instead shunting pyruvate toward glycolysis (50, 54). This in turn increases the cell's glycolytic flux and lowers ROS production. It appears that UCP2 effectively applies a "brake" on pyruvate entry into the mitochondria in order to reduce ROS production in glycolytic cells, such as PSCs, cancer cells, and ischemic cells (90). Several studies have also found that UCP2 is associated with increased proton leak in which the cell uncouples oxygen consumption with ATP production in order to lower the mitochondrial membrane potential (90-93). This in turn lowers ROS production from the ETC. Therefore, UCP2 may play two potential roles in mESCs: (1) preventing pyruvate uptake by the mitochondria; and (2) acting as an uncoupling agent in the mitochondrial respiratory chain. Although more research is required to understand the exact mechanism by which UCP2 acts, studies thus far have demonstrated that UCP2 promotes high glycolytic flux

and lowers ROS production in mESCs; therefore, UCP2 acts as a key regulator of pluripotency in mESCs.

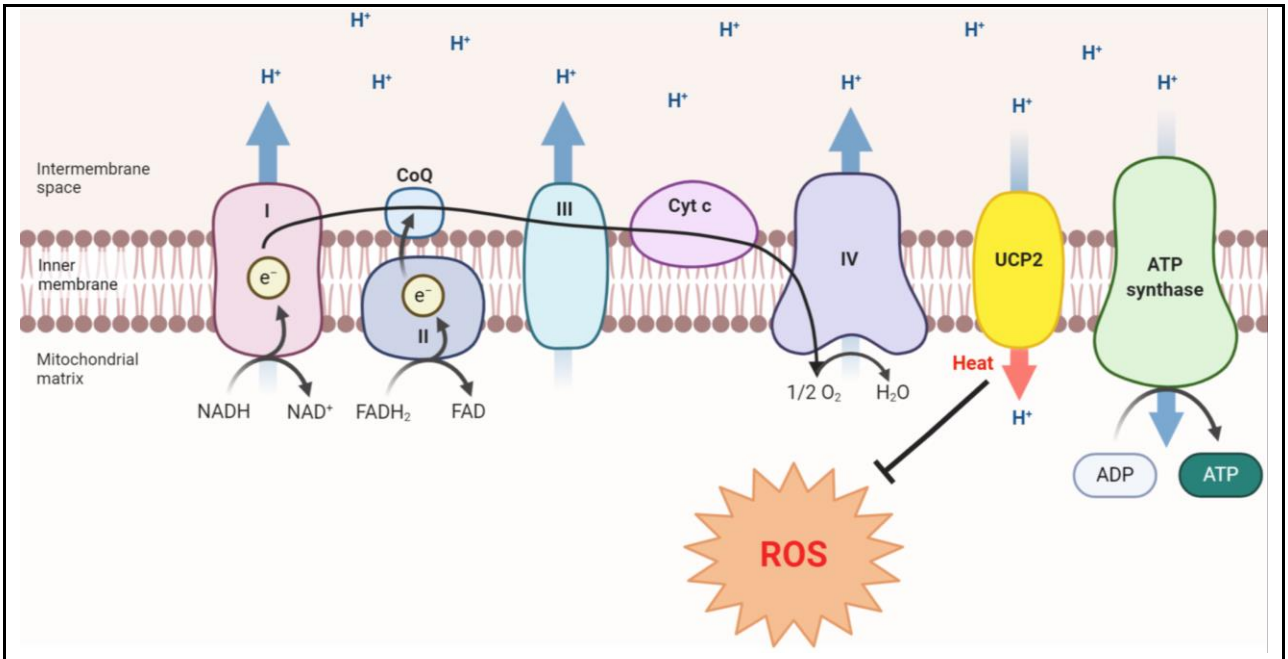

Figure 1.5 Uncoupler protein 2 (UCP2) is critical for maintenance of the pluripotent state. UCP2 promotes high glycolytic flux and reduces ETC activity in order to minimize ROS production in PSCs. Created with BioRender.com.

1.8 Significance

1.8.1. Significance

TMAO has been shown to be an independent biomarker for many different chronic diseases, including atherosclerosis, Alzheimer's Disease, stroke, chronic kidney disease, and diabetes (20, 23, 26). Additionally, it directly effects several different cell types, including endothelial cells, neurons, macrophages, and vascular smooth muscle cells by inducing inflammatory pathways and ROS generation (3, 4, 6, 7). The purpose of my research project is to

determine whether TMAO will (1) impact mESC viability, proliferation, and potency; and (2) impact mESC metabolism. As discussed earlier, mESCs are derived from the ICM of the pre-implantation blastocyst and are exposed to metabolites circulating the mother's bloodstream via endometrial secretions (39). If TMAO negatively impacts the viability, proliferation, or differentiation ability of the cells at this critical stage in early embryonic development, then likely it will result in early embryonic lethality (43). Next, this review thoroughly discusses the strong interplay between pathways which regulate metabolism and those that regulate potency. TMAO has been shown in several cell types to cause damage through increased oxidative stress, and many stem cells types are highly sensitive to ROS (3, 6, 31). Further, ROS acts as a signaling molecule that triggers metabolic remodeling and the onset of differentiation in stem cells (79, 80). Therefore, in my project I wanted to explore the potential impact of TMAO on mESC metabolism, as this would indicate whether TMAO could cause premature differentiation or senescence in stem cells via modulation of metabolic activity. Many different studies have demonstrated the similarities between PSCs and adult stem cells in their metabolic activity and tight regulation of redox signaling (2, 57-59). Therefore, this study is important not only for investigating the impact of TMAO on mESCs, but also for providing insight into how TMAO may impact adult stem cell populations which are critical for the maintenance and repair of tissues throughout the human life span.

CHAPTER TWO: TRIMETHYLAMINE N-OXIDE DECREASES MOUSE EMBRYONIC STEM CELL POTENCY POTENTIALLY VIA MODULATION OF METABOLIC PATHWAYS

2.1 Abstract

Trimethylamine N-oxide (TMAO) is a metabolite derived from dietary choline, betaine, and carnitine via gut microbial metabolism. In several recent studies, TMAO has been shown to directly induce inflammation and reactive oxygen species (ROS) generation in numerous cell types, resulting in cell dysfunction. However, whether TMAO will impact stem cell properties remains unknown. This project aims to explore the potential impact of TMAO on mouse embryonic stem cells (mESCs), which serve as an in vitro model of the early embryo and of other potent stem cell types. Briefly, mESCs were cultured in the absence (0mM) or presence of TMAO under two different sets of treatment conditions: long-term (21 days), low-dose (20μM, 200μM, and 1000μM) treatment or short-term (5 days), high-dose (5mM, 10mM, 15mM) treatment. Under these treatment conditions, mESC viability, proliferation, and stemness were analyzed. mESC properties were not negatively impacted under long-term, low-dose TMAO treatment; however, short-term, high-dose treatment resulted in significant reduction of mESC viability and proliferation. Additionally, mESC stemness was significantly reduced when high-dose treatment was extended to 21 days. To investigate an underlying cause for TMAO-induced loss in mESC stemness, metabolic activity of the mESCs under short-term, high-dose TMAO treatment was measured with a Seahorse XFe96 Analyzer. TMAO treatment significantly decreased the rate of glycolysis and increased the rate of compensatory glycolysis upon inhibition of oxidative phosphorylation (OxPHOS). Additionally, it significantly increased the rate of OxPHOS, maximal respiratory capacity, and respiratory reserve. These findings indicate

that TMAO induced a metabolic switch of mESCs from high glycolytic activity to greater OxPHOS activity to promote their differentiation. Additionally, TMAO resulted in increased proton leak, indicating increased oxidative stress, and elucidating a potential underlying mechanism for TMAO-induced loss in mESC stemness. Altogether, these findings indicate that TMAO decreases stem cell potency potentially via modulation of metabolic activity.

2.2 Introduction

Trimethylamine N-oxide (TMAO) has recently entered the limelight as a small metabolite that appears to provide a strong link between diet and negative health outcomes (26). TMAO is derived from gut microbial metabolism of dietary components, such as choline, carnitine, and betaine which are obtained from foods such as red meat and eggs (4, 11, 13, 14). High plasma TMAO levels are highly associated with a host of chronic diseases, including atherosclerosis, Alzheimer's Disease, diabetes, chronic kidney disease, and stroke (4, 5, 20, 23, 27). Several recent studies have shown that TMAO directly induces dysfunction in several cell types via induction of inflammatory markers and reactive oxygen species (ROS) production (3, 6, 31). Stem cells are particularly sensitive to increased ROS generation, because it serves as a regulator of mESC viability, proliferation, and potency (79, 80). As a result, stem cells have evolved mechanisms to prevent excessive ROS production, including the generation of high levels of antioxidants through a highly active pentose phosphate pathway (PPP), and maintaining low levels of ROS generation through reduced activity of the electron transport chain (ETC). Additionally, mESCs rely mostly on aerobic glycolysis for ATP production, rather than oxidative phosphorylation (OxPHOS), in order to generate the intermediary metabolites required for anabolic pathways that support their high proliferation rate (1). Therefore, the metabolic phenotype of mESCs plays a key role in tightly regulating redox balance and in the maintenance

of mESC properties. When the redox balance is upset, it can trigger the modulation of mESC metabolic activity, and subsequent loss of mESC viability and pluripotency (55). Therefore, it is important to determine whether TMAO will impact mESC metabolic activity and properties through increased oxidative stress. These cells, which are derived from the inner cell mass of the pre-implantation blastocyst, serve as a model of a critical stage of early embryonic development in which perturbations to mESC properties can result in early embryonic lethality (43). Additionally, many pathways regulating metabolism and potency in mESCs are shared with adult stem cells, and thus, this study may provide insight into how long-term TMAO exposure in adults may impact resident stem cell populations and contribute to the onset of chronic and aging-related diseases (2).

The objective of this study was to determine whether TMAO will impact mESC viability, proliferation, and stemness under two separate treatment conditions: a long-term (21 days), low-dose (20μM, 200μM, and 1000μM) treatment; and a short-term (5 days), high-dose (5mM, 10mM, 15mM) treatment. We then examined whether TMAO will impact mESC metabolic activity under the high dose treatment condition using a Seahorse XFe96 Analyzer, which provided measurements of oxygen consumption rate (OCR) and extracellular acidification rate (ECAR) under different experimental conditions. These metabolic measurements provided information on glycolytic vs OxPHOS activity in the mESCs, as well as potential signs of oxidative stress on the cell through increased proton leak.

2.3 Overall Experimental Design

In this project, I explored whether TMAO may impact the properties of mESCs through increasing mitochondrial dysfunction. To test this, I performed two sets of cell treatment with TMAO: (1) long-term, low dose treatment; and (2) short-term, high dose treatment. For long-

term treatment, the length of treatment was 21 days, because this is the length of mouse gestation. Although mESCs are not present for the entire length of mouse gestation, there are stem cells with relatively high levels of potency all throughout mouse gestation. The range of concentrations chosen for the low dose treatment were based on concentrations of TMAO seen in healthy female mice (20 μM) and mice fed a western diet high in TMAO (200 μM), with 1000 μM being at the high end. For short-term treatment, 5 days was chosen, because mESCs cannot be cultured in a plate for longer than 5 days. After 5 days, they must be passaged in order to maintain their quality and health. It is not ideal to detach and replate cells undergoing treatment with high concentrations of TMAO, because dying cells in the dish will not reattach during the replating process. Therefore, in order to provide a more accurate representation of TMAO's impact on viability and proliferation, we selected a 5-day treatment so that experiments could be performed directly in the dish on Day 5. The range of concentrations for the high dose treatment were chosen based on results from Calcein-AM and ATP-based viability assays. 5mM and 10mM TMAO treatment resulted in small decreases in mESC viability, whereas 15mM TMAO treatment resulted in a drastic decrease in mESC viability. As a result, 5-day experiments were carried out with 0mM, 5mM, and 10mM TMAO treatment, and some also included 15mM as the highest dose in the range of TMAO treatments as a positive control for TMAO-induced negative effects.

After the mESCs were exposed to both sets of TMAO treatments, I measured their viability with a Calcein-AM and ethidium homodimer-1 (EthD-1)-based assay, proliferation with an EdU-based cell proliferation assay, and stemness with an antibody-based immunocytochemistry assay. Next, I used the Seahorse XFe96 Analyzer to measure the metabolic activity of the mESCs after short-term, high-dose TMAO treatment, in order to

determine the extracellular acidification rate (i.e., rate of glycolysis) and the rate of oxygen consumption (i.e., rate of mitochondrial oxidative phosphorylation). These experiments also provided information about the cell's compensatory glycolysis, maximal respiratory capacity, respiratory reserve, and proton leak under different concentrations of TMAO, compared to the control.

2.4 Materials and Methods

2.4.1 Reagents

All chemicals used in the present study are listed below unless otherwise stated elsewhere: Antimycin-A (AMA, Sigma-Aldrich, St. Louis, MO), anti-stage specific embryonic antigen-1 (SSEA-1, Santa Cruz Biotech, Dallas, TX), Calcein-AM & Ethidium homodimer-1 (EthD-1, both from Thermo Fisher Scientific), carbonylcyanide p-trifluoromethoxyphenylhydrazone (FCCP, Sigma-Aldrich, St. Louis, MO), Click-iT 5-ethynyl-2'-deoxyuridine (EdU) Proliferation kit (Life Technologies, Carlsbad, CA), ES-cell qualified fetal bovine serum (FBS, ZenBio, Research Triangle, NC), glucose (Sigma-Aldrich, St. Louis, MO), L-glutamine (Quality Biological Inc), high glucose Dulbecco's Modified Essential Medium (DMEM, GE Healthcare Life Sciences, Pittsburgh, PA), Hoechst 33342 (Thermo Fisher Scientific, Waltham, MA), leukemia inhibitory factor (LIF, PeproTech, Rocky, NJ), nonessential amino acids (NEAA, Quality Biological Inc., Gaithersburg, MD), oligomycin (Sigma-Aldrich, St. Louis, MO), 1X Penicillin/Streptomycin (P/S,VWR, Radnor, PA), 2-deoxy-glucose (2-DG, Sigma-Aldrich, St. Louis, MO), and 2-mercaptoethanol (2-ME, Sigma-Aldrich, St. Louis, MO).

2.4.2 mESC Culture

The mouse embryonic stem cell (mESC) line C57BL/6 purchased from the American Type Culture Collection (ATCC, Cat. SCRC-1002, Manassas, VA) was cultured in 0.1% gelatin-coated plates at 37^{o}C, 21%O_2 and 5%CO_2 with high glucose DMEM consisting of 15% ES-cell qualified FBS, 1000 U/ml LIF, 0.1 mM NEAA, 0.1 mM 2-ME, 2 mM L-glutamine, and 1X penicillin streptomycin with daily medium change. Cells were passaged every 3-5 days or when they reached 90% confluency.

2.4.3 Live/Dead Assay with Calcein-AM/EthD-1 and Hoechst 33342 staining

Cells were plated at a density of 2.5e4 cells per well on a gelatin-coated 12-well plate, and were cultured with different TMAO concentrations (0 µM, 20 µM, 200 µM, 1000 µM) until their viability was examined on Day 21. Afterward, cells were washed 1X with phosphate buffered saline (PBS) and incubated with 2 µM Calcein-AM, 1.25 µM EthD-1 (both are from Thermo Fisher Scientific), and 1µM Hoechst 33342 for 20 minutes. Only live cells with intracellular esterase activity could digest non-fluorescent calcein-AM into fluorescent calcein. Dead or dying cells containing damaged membranes allowed the entrance of EthD-1 to stain the nuclei. Cells were imaged with an Olympus IX73 microscope equipped with a DP70 CCD camera (Olympus, Center Valley, PA). The images were then analyzed using ImageJ software (NIH). At least 800 Hoechst cells were analyzed in each group to calculate % of dead cells over total number of cells.

2.4.4 ATP-based Viability Assay

Cells were plated at a density of 8e3 cells per well on a gelatin-coated 96-well plate for 5 days with different TMAO concentrations (0mM, 5mM, 10mM, 15mM). On Day 5, cells were detached and counted. 5e3 cells from each treatment group were added to a luminometer plate

and treated with 100µL of nucleotide release buffer for 5 minutes at room temperature with gentle shaking according to the manufacturer's protocol. Then 10µL of ATP Monitoring Enzyme was added to the cell lysates, and luminescence of the samples was measured within 1 minute using SpectraMax M5 plate reader (Molecular Devices, Sunnyvale, CA). ATP contents were normalized by the control group (0mM TMAO) and reported as percentages.

2.4.5 EdU Cell Proliferation Assay

Cells were plated at a density of 2.5e4 cells per well on a gelatin-coated 12-well plate. Cell proliferation was examined on Days 5 and 21, depending on the treatment type they received. Briefly, cells were incubated with 1X EdU for 2.5 hours, and then washed with PBS to stop the reaction. The cells were detached with TryplE, fixed with 4% paraformaldehyde (PFA) at room temperature (RT) for 30 minutes, and then cytospun onto glass tissue slides at 1100 revolutions per minute (RPM) for 4 minutes. The cells were then stained by following the manufacturer's protocol included in the Click-iT EdU Cell Proliferation kit. After co-staining with Hoechst 33342, fluorescent EdU images were taken with Olympus IX73 microscope mentioned above and analyzed using ImageJ software. At least 800 Hoechst cells were analyzed in each group to calculate % of EdU positive cells over total number of cells (Hoechst staining).

2.4.6 Stemness Assay with Immunocytochemistry

Cells were plated at a density of 5e4 cells per well on a gelatin-coated 6-well plate. Cell stemness was examined on Days 5 and 21, depending on the treatment type they received. Cells were detached with TryplE, fixed with 4% PFA at RT for 30 minutes, and then cytospun onto glass tissue slides at 1100 RPM for 4 minutes. The resulting cells were then washed 2X with

PBS, followed by blocking in 1.5% bovine serum albumin (BSA) and 0.2% Tween20 buffer for 1 hour at RT. After that, cells were incubated overnight with 1:250 anti-SSEA-1, washed 3X, and stained with a secondary antibody, goat anti-mouse 594, at a concentration of 1:1000 in blocking buffer. An additional set of coverslips were stained with only secondary antibody as a negative control, and Hoechst 33342 was counterstained to label cell nuclei in all groups. Fluorescent images were taken with Olympus IX73 microscope mentioned above and analyzed using ImageJ software. At least 1,000 Hoechst cells were analyzed in each group to calculate % of SSEA-1-positive cells over total number of cells (Hoechst staining).

2.4.7 Measurement of Extracellular Acidification Rate with Seahorse

Extracellular acidification rate (ECAR) of mESCs after exposure to TMAO was determined using a Seahorse XFe96 Analyzer (Agilent Technologies Mississauga, ON). mESCs were cultured for 5 days in different concentrations of TMAO (0mM, 5mM, 10mM). On Day 5, cells were detached and replated at a density of 1e5 cells in Seahorse 96-well cell culture microplates, coated with 0.1% gelatin. They were allowed 2 hours to attach to the plate before beginning ECAR measurements. This was done to ensure that each well had the same number of cells. Following incubation, cells were washed with serum-free, bicarbonate-free, Seahorse base medium (supplemented with 2mM L-glutamine) twice and then immersed in a total volume of 180µL of media in each well immediately before the assay. The Seahorse XFe96 Analyzer uses solid-state probes to measure the increase in the proton concentration of cell media at programmed intervals providing measures of ECAR in mpH/min under experimental conditions. During the Seahorse assay, metabolism can be manipulated by injecting reagents to inhibit components of glycolysis and OxPHOS, altering ECAR from the ‘resting’ basal conditions as

shown in Figure 2.1. The glycolysis stress kit was used to measure ECAR response following addition of glucose (10 mM), oligomycin (1 μM), and 2-DG (100 mM) (see Figure 2.1A). Following each injection, five measurements were taken. The average ECAR measurement after addition of glucose provides a baseline measurement of glycolysis. Addition of oligomycin inhibits the activity of F_1F_0ATP synthase (ATPase), providing a measure of compensatory glycolysis, which is defined as the (average ECAR post-oligomycin injection) – (average ECAR post-glucose injection before the addition of oligomycin). 2-DG is a glucose analog that inhibits hexokinase, the first enzyme in the glycolysis pathway, and thus, the average ECAR measurement after injection of 2-DG provides a measurement of non-glycolytic acidification (94).

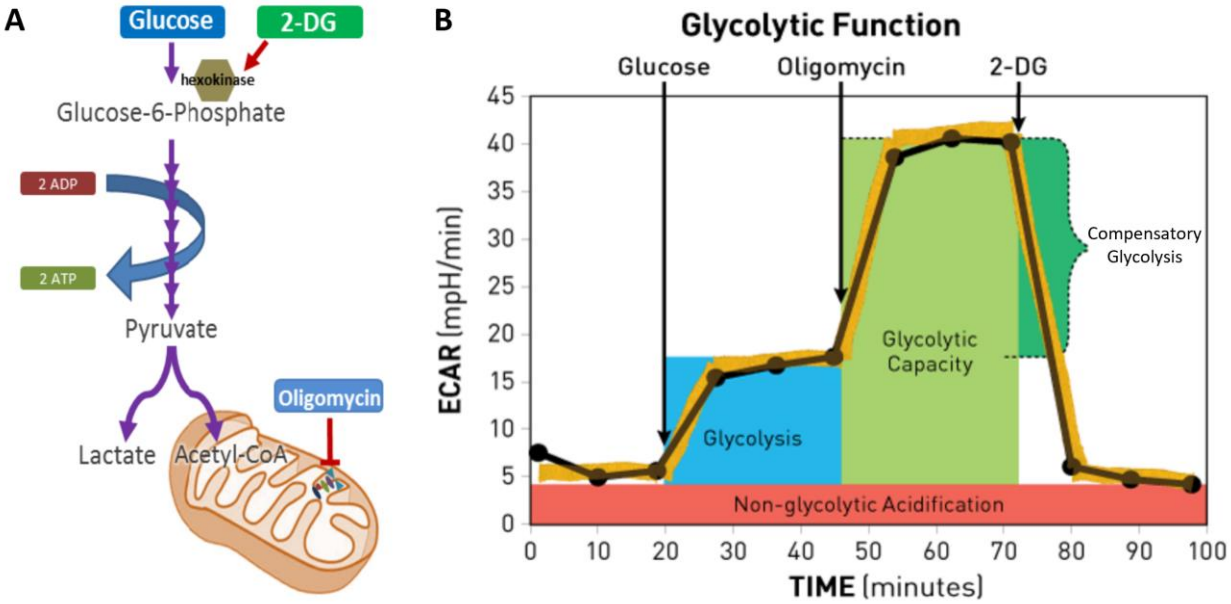

Figure 2.1 Schematic of glycolysis stress test measurements and chemical components: (a) Addition of chemical compounds, glucose, oligomycin, and 2-DG, influence glycolytic and OxPHOS activity, and (b) measurement of ECAR before and after the injection of these chemical compounds provides the rate of non-glycolytic acidification, baseline rate of glycolysis, and compensatory glycolysis. Images reproduced with Permission, Courtesy of © Agilent Technologies, Inc.

2.4.8 Measurement of Mitochondrial Oxygen Consumption Rate with Seahorse

Oxygen consumption rate (OCR) of mESCs was determined using a Seahorse XFe96 Analyzer (Agilent Technologies Mississauga, ON). mESCs were cultured for 5 days in different concentrations of TMAO (0mM, 5mM, 10mM). On Day 5, cells were detached and replated at a density of 1e5 cells in Seahorse 96-well cell culture microplates, coated with 0.1% gelatin. They were allowed 2 hours to attach to the plate before beginning OCR measurements. This was done

to ensure that each well had the same number of cells. Following incubation, cells were washed with serum-free, bicarbonate-free, Seahorse OCR assay medium (1mM pyruvate, 2mM glutamine, and 10mM glucose) twice and then immersed in a total volume of 180µL of media in each well immediately before the assay. Plates were then placed in the XFe96 Analyzer to establish a basal level of respiration. The Seahorse XFe96 Analyzer uses solid-state probes to measure the decline in the oxygen concentration of cell media at programmed intervals providing measures of oxygen consumption rate (OCR) in pmol/min under experimental conditions. During a Seahorse assay, metabolism can be manipulated by injecting reagents to inhibit components of the ETC, altering OCR from the 'resting' basal conditions as shown in Figure 2.2. The mitochondrial stress test included the addition of oligomycin (1 µM), FCCP (4 µM), and AMA (1 µM) in order to assess mitochondrial function as shown in Figure 2.2A. Following each injection, five measurements were taken. The addition of antimycin A inhibits complex III and ultimately stops ETC-mediated OCR, therefore, the average OCR after antimycin A injection provides non-mitochondrial respiration. Basal respiration was defined as (the average OCR prior to injections) – (non-mitochondrial respiration). Oligomycin inhibits the activity of ATPase providing a measure of OCR not coupled to ATP production. FCCP is a protonophore that acts to uncouple the established proton gradient across the mitochondrial membrane. FCCP uncoupling causes the ETC to consume oxygen at a maximal rate to provide maximal OCR capacity measurements. Proton leak was defined as (minimum OCR measurement post-oligomycin injection before the injection of FFCP) – (non-mitochondrial respiration). Maximal respiration was calculated as (maximal OCR measurement after the injection of FCCP) – (non-mitochondrial respiration). Reserve capacity was calculated as (maximal respiration) – (basal respiration) (94).

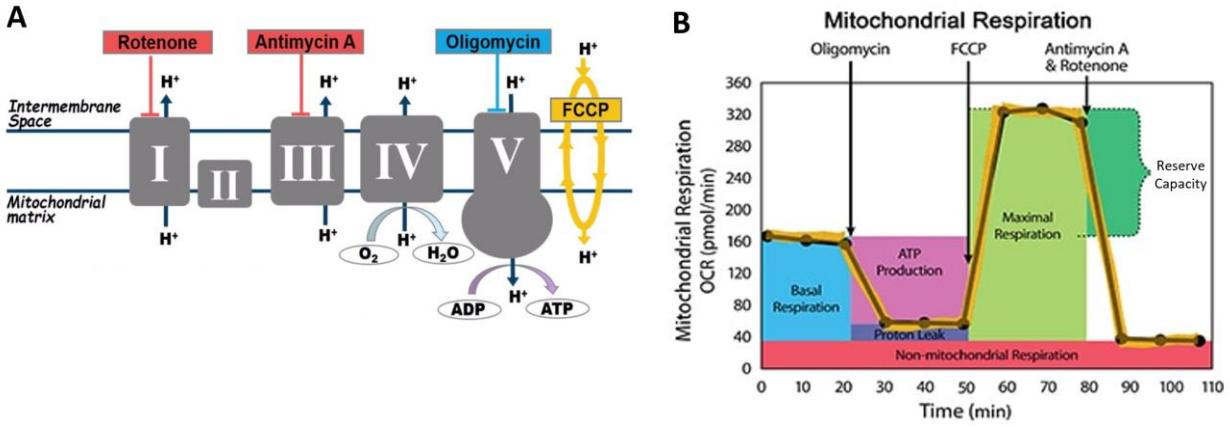

Figure 2.2 Schematic of mitochondrial stress test measurements and chemical components: (a) Addition of chemical compounds, AMA, oligomycin, and FCCP, influence OxPHOS activity, and (b) measurement of OCR before and after the injection of these chemical compounds provides the rate of basal respiration, maximal respiratory capacity, reserve capacity, and proton leak. Images reproduced with Permission, Courtesy of © Agilent Technologies, Inc.

2.4.9 Statistical Analysis

All experiments were performed at least three times with at least three replicates per group, unless otherwise noted. All data are shown as mean ± standard error (SE). Student's *t*-test with a two-tailed distribution was used to compare two groups. One-way analysis of variance (ANOVA) followed by the tukey test was used to compare three or more groups with $p < 0.05$ being considered statistically significant. GraphPad Prism 5 and Microsoft Excel 2016 were used for statistical analysis and plotting.

2.5. Results

2.5.1. TMAO does not Impact mESC Viability, Proliferation, and Stemness Under Physiological Conditions

To determine whether TMAO may impact the overall health of mESCs, I first examined its effect on viability, proliferation, and stemness under physiological conditions. Viability was assessed with a LIVE/DEAD assay. Briefly, mESCs were cultured for 21 days with TMAO at different concentrations (0μM, 20μM, 200μM, 1000μM). Cells were passaged every 3-5 days, and the final passage before Day 21, the cells were plated in 12-well plates. On Day 21, the cells were co-stained with Calcein-AM, EthD-1, and Hoechst 33342, and then imaged with a fluorescent microscope. Quantitative analysis shows no statistically significant differences between the control and TMAO-treated groups in terms of cell viability (% of live cells are 97%±1.5 in control vs 96%±1.7 in 20μM, 97%±0.71 in 200μM, and 98%±0 in 1000μM, n=3 in all groups, ns, Figure 2.3B). Thus, TMAO does not impact mESC viability under physiological conditions.

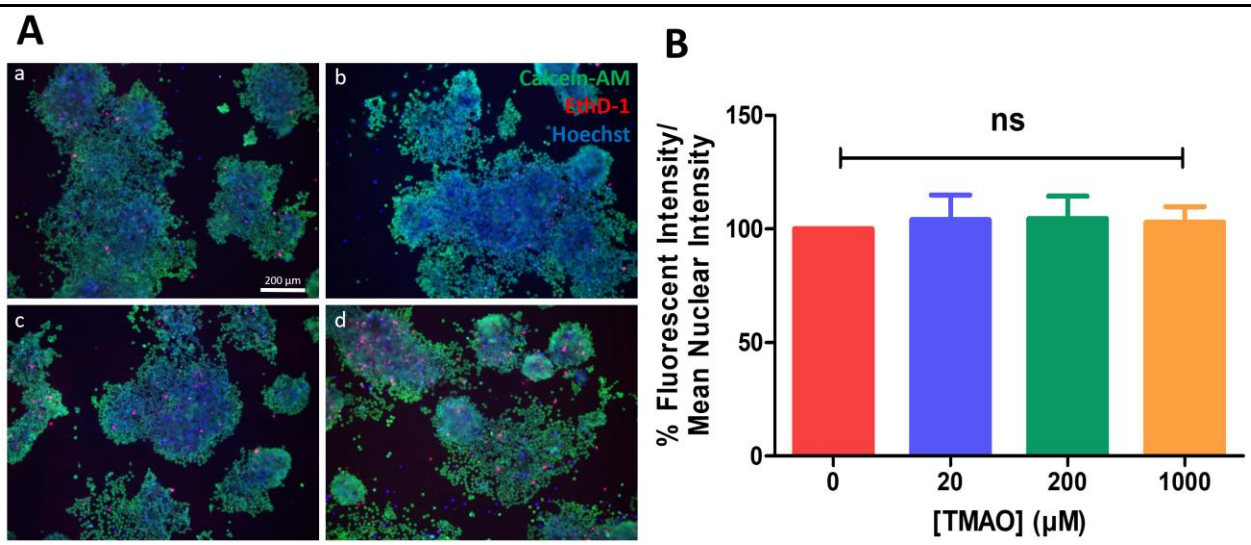

Figure 2.3 mESCs maintain viability under long-term, low-dose TMAO treatment. **A.** The representative images of mESCs stained with Calcein-AM (green), EthD-1 (red), and Hoechst (blue) after 21 Days of treatment with (a) 0µM, (b) 20µM, (c) 200µM and (d) 1000µM TMAO. Scale bar=200µm. **B.** The % of EdU positive cells. ns: not significant; n=3.

In order to quantitatively analyze the effect of TMAO on cell proliferation, I performed both an EdU assay and a cell doubling time (DT) assay. For the cell DT assay, I cultured the cells for 21 days with TMAO at different concentrations (0µM, 20µM, 200µM, 1000µM). Cells were passaged every 3-5 days and the cell number was counted at each passage. DT was calculated using the following formula: $DT=(t_2-t_0)\log 2/(\log N_2-\log N_0)$ where t_2, t_0 indicate time points at counting and initial plating, respectively; and N_2, N_0 indicate number of cells at respective time points (95). As shown in Figure 2.4C, the cell DT did not differ significantly for the 3 different groups of TMAO-treated mESCs compared to the control (cell doubling times are 14.8 hours±2.0 in control vs 15.3 hours±2.6 in 20µM, 15.3 hours±2.3 in 200µM, and 16.7 hours±3.5 in 1000µM, n=3 in all groups, ns). I next performed an EdU assay to quantitatively

analyze cell proliferation. EdU is a nucleoside analog of thymidine and is incorporated into DNA during synthesis. The EdU contains an alkyne, which undergoes a click reaction with an azide that is contained in the Alexa Fluor dye, which allows for fluorescent labeling of newly synthesized DNA, so that cell proliferation can be quantified. Briefly, cells were passaged every 3-5 days, and the final passage before Day 21, the cells were plated in 96-well plates. On Day 21, the cells were incubated for 2.5 hours with EdU. Then they were washed 1X with PBS, detached, fixed with 4% PFA, cytospun onto coverslips, and then co-stained with Alexa Fluor azide and Hoechst 33342. The stained coverslips were flipped over and mounted on tissue slides and microscopic fluorescent images were taken from the bottom of the slides using the Olympus IX73 microscope mentioned above. As indicated from Figure 2.4B, there were no statistically significant differences between the control and TMAO-treated groups in terms of cell proliferation (% of EdU positive cells are 62%±6.2 in control vs 65%±5.2 in 20µM, 66%±6.5 in 200µM, and 65%±4.3 in 1000µM, n=3 in all groups, ns). Thus, TMAO does not impact mESC proliferation under physiological conditions.

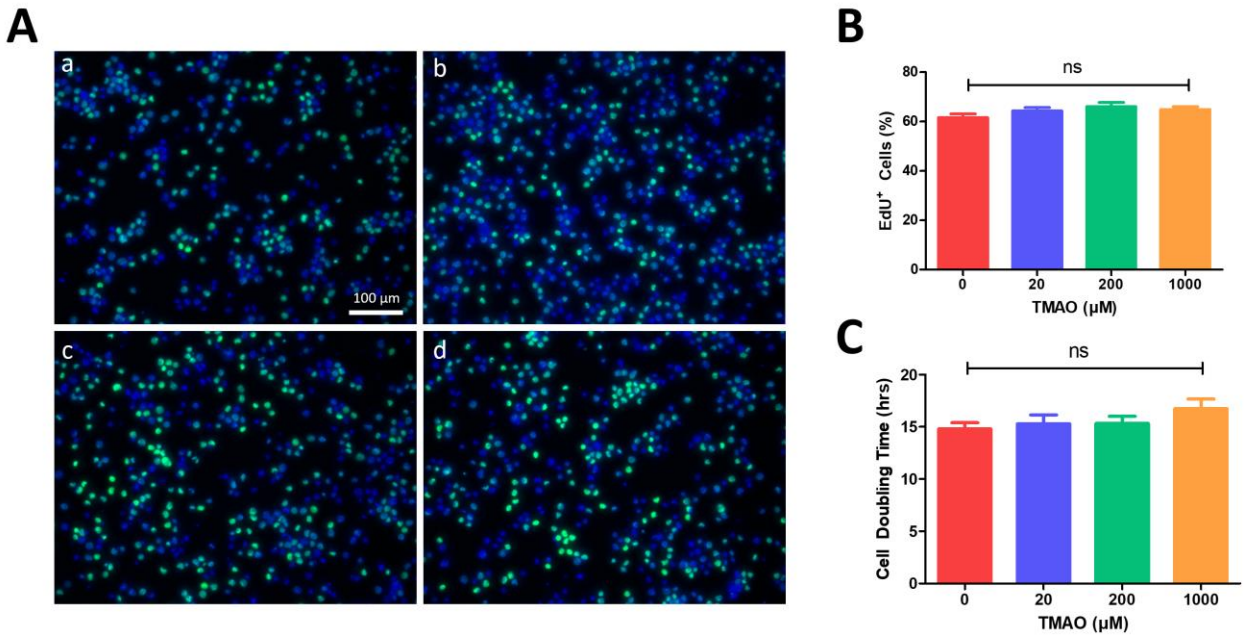

Figure 2.4 mESCs maintain proliferation rate under long-term, low-dose TMAO treatment. **A.** The representative images of mESCs stained with EdU (green) and Hoechst (blue) after 21 Days of treatment with (a) 0µM, (b) 20µM, (c) 200µM and (d) 1000µM TMAO. Scale bar=100µm. **B.** The % of EdU positive cells. ns: not significant; n=3. **C.** The cell doubling time. ns: not significant; n=5.

To determine whether TMAO will impact mESC stemness, I performed immunocytochemistry with anti-SSEA-1 antibody, a pluripotency marker. Briefly, mESCs were cultured for 21 days without TMAO or with 1000µM TMAO. Cells were passaged every 3-5 days. On Day 21, the cells were detached, fixed with 4% PFA, cytospun onto coverslips, and then co-stained with anti-SSEA-1 antibody and Hoechst 33342. The stained coverslips were flipped over and mounted on tissue slides and microscopic fluorescent images were taken from the bottom of the slides using the Olympus IX73 microscope mentioned above. As indicated

from Figure 2.5B, no statistically significant differences were found between the control and TMAO-treated groups in terms of cell stemness (% of SSEA-1 positive cells are 91%±6.0 in control vs 89%±2.6 in 1000μM, n=5 in all groups, ns). Thus, at these physiological concentrations, TMAO does not impact mESC viability, proliferation, and stemness.

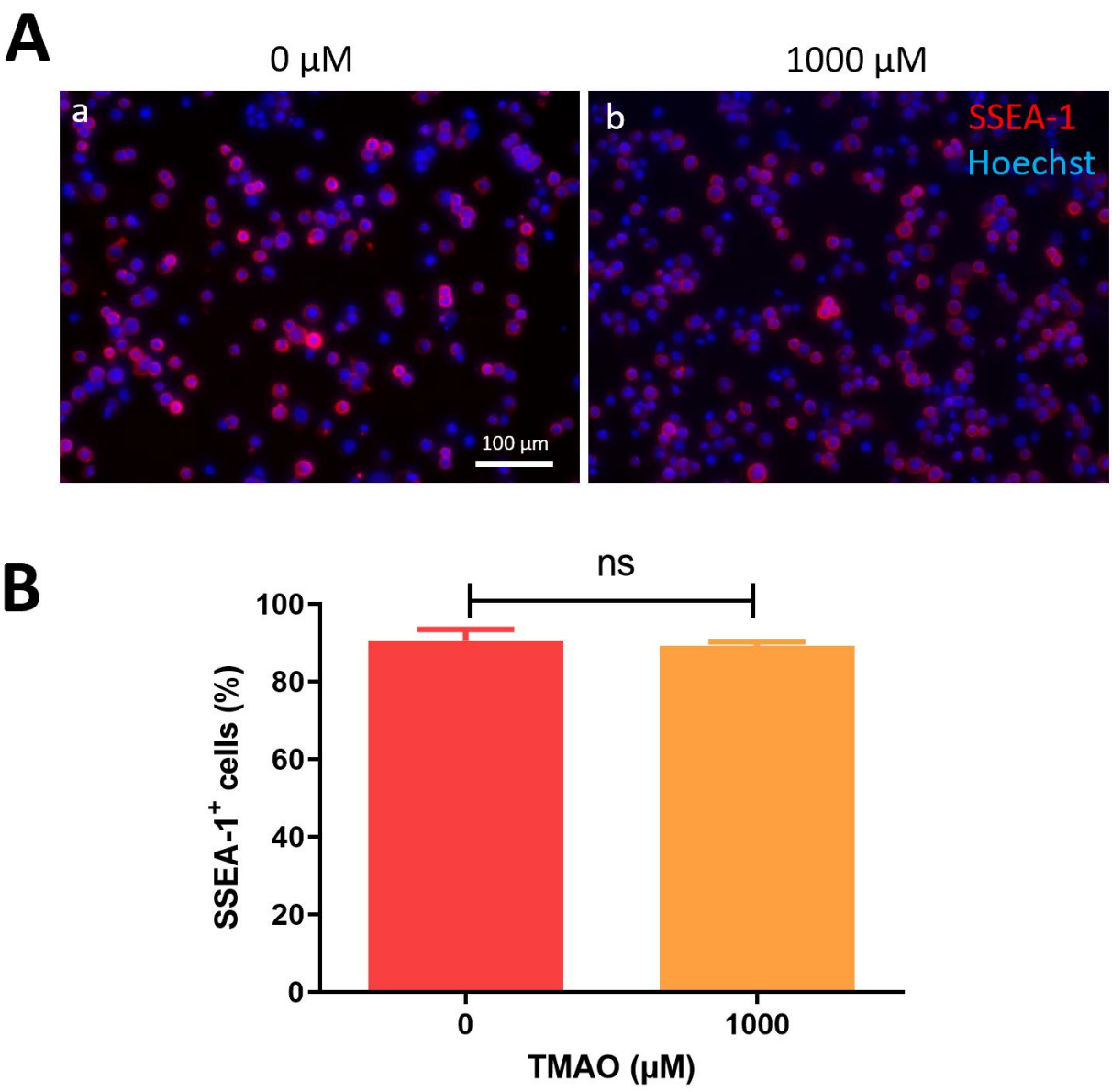

Figure 2.5 mESCs maintain stemness under long-term, low-dose TMAO treatment. **A.** The representative images of mESCs stained with anti-SSEA-1 (red) antibody and Hoechst (blue) after 21 Days of treatment with (a) 0µM and (b) 1000µM TMAO. Scale bar=100µm. **B.** The % of SSEA-1 positive cells. ns: not significant; n=5.

2.5.2. High Concentrations of TMAO Lead to Decrease in mESC Viability, Proliferation, and Stemness

To determine the concentration at which TMAO will have an impact on mESC viability, a preliminary viability assay was performed with a Calcein-AM stain after 5 days of exposure to high concentrations of TMAO (5mM, 10mM, and 30mM). On Day 5, the cells were stained with Calcein-AM, and fluorescent images were taken using the Olympus IX73 microscope mentioned above with the 4X objective, so that the entire well could be captured for each treatment group for gross calculation of the total green area in mm^2, which represents the area of viable cells in each well. This assay helped to broadly determine a range at which TMAO will significantly decrease mESC viability: (area of green in mm^2 for control group is $27mm^2 \pm 5.8$ vs $27mm^2 \pm 6.0$ in 5mM, $23mm^2 \pm 5.3$ in 10mM, and $11mm^2 \pm 1.6$ in 30mM, n=3, *:$p<0.05$, **: $p<0.01$, Figure 2.6).

Based on the Calcein-AM assay, a range of TMAO concentrations were selected to perform more sensitive assays, including an ATP viability assay, an EdU proliferation assay, and immunocytochemistry-based stemness assay. These assays were performed in order to investigate the impact of short-term, high doses of TMAO on mESC overall health.

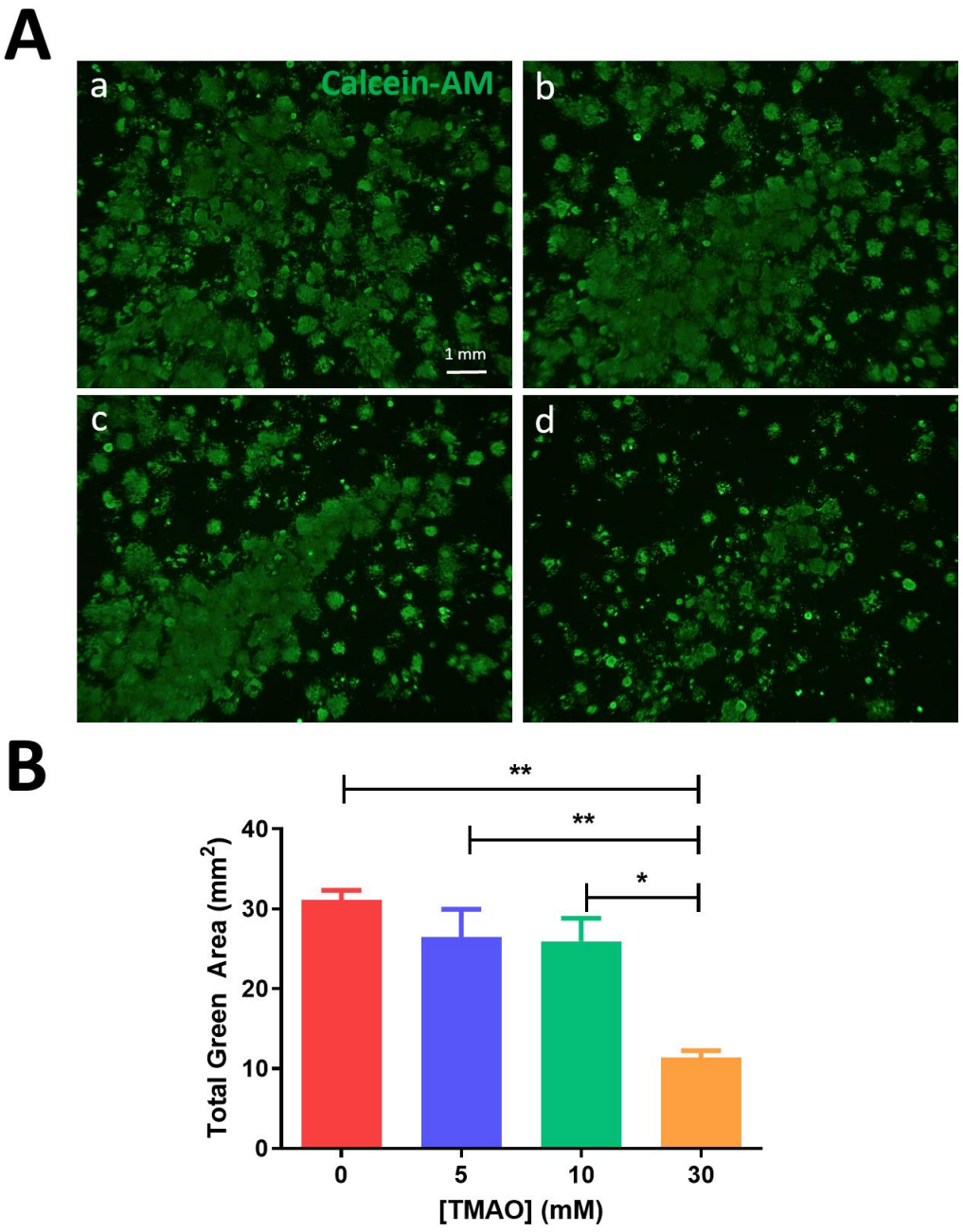

Figure 2.6 mESC viability after treatment with wide range of high TMAO concentrations. **A.** The representative images of mESCs stained with Calcein-AM (green) after 5 Days of treatment with (a) 0mM, (b) 5mM, (c) 10mM, and (d) 30mM TMAO. Scale bar=1mm. **B.** Total green area in mm^2. *:$p<0.05$, **: $p<0.01$; n=3.

Decrease in ATP level is an indication of cell death and can be measured with an ApoSENSOR Cell Viability Assay Kit, which utilizes luciferase to catalyze the formation of light from the reaction of ATP and luciferin. Briefly, the mESCs were cultured for 5 days at high concentrations of TMAO (0mM, 5mM, 10mM, 15mM), then detached, lysed, and transferred to a 96-well plate for analysis using a plate reader. The percent decrease in ATP levels was calculated by comparing the relative fluorescent units (RFU) of the treatment groups to the control. The ATP assay demonstrated that mESC viability decreased significantly with treatment of high concentrations of TMAO (ATP % of control is 85%±11 in 5mM, 82%±15 in 10mM, and 63%±14 in 15mM, n=3, *:$p<0.05$, **: $p<0.01$, ****:$p<0.0001$, Figure 2.7).

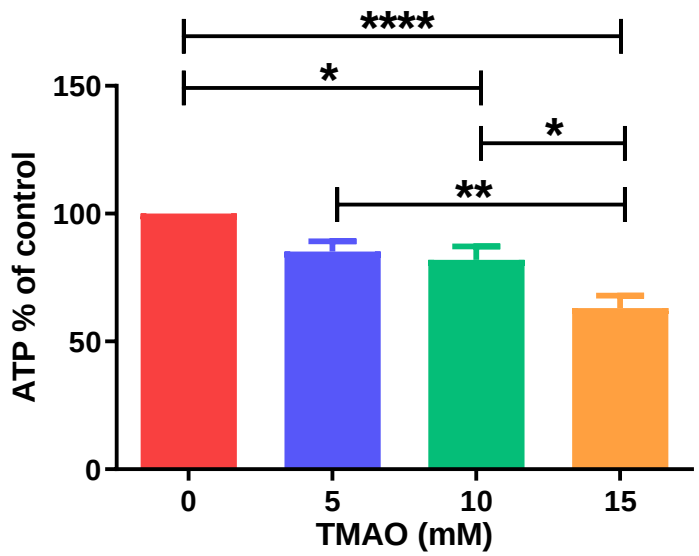

Figure 2.7 mESC viability decreases under short-term, high-dose TMAO treatment. Viability represented as percent of ATP content in the TMAO-treated groups compared to the control. *:p<0.05, **: p<0.01, ****: p<0.0001; n=3.

Cell proliferation was analyzed using the EdU assay described above, after 5 days of the high dose TMAO treatment (0mM, 5mM, 15mM) described above. Proliferation was calculated as the mean intensity of the area of EdU positive cells divided by the mean intensity of total nuclei. Quantitative analysis demonstrated that mESC proliferation decreased significantly with the high concentrations of TMAO (Mean intensity of EdU+ cells/mean intensity of nuclei is 1880±128 in control vs 1360±220 in 5mM, and 1250±85 in 15mM, n=3, *: p<0.05, **:p<0.01, *:p<0.0001 Figure 2.8B).

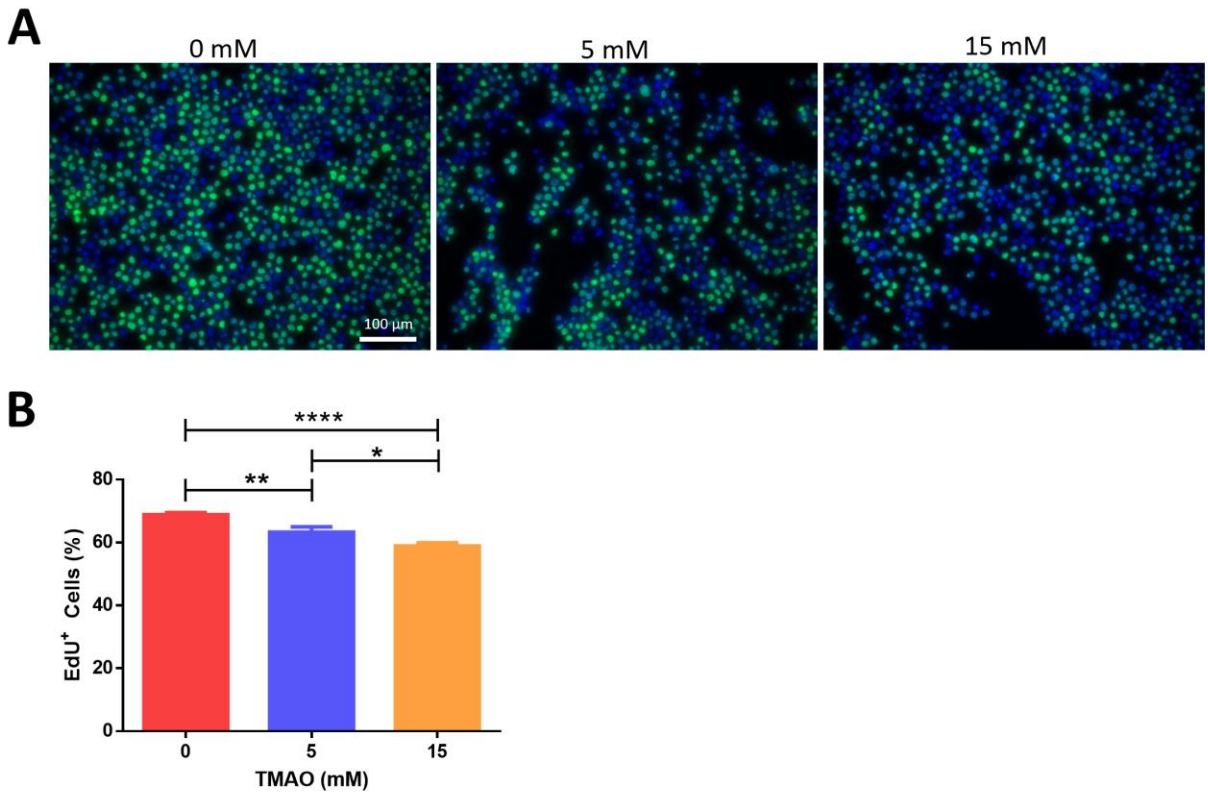

Figure 2.8 mESC proliferation rate decreases under short-term, high-dose TMAO treatment. **A.** The representative images of mESCs stained with EdU (green) and Hoechst (blue) after 5 Days of treatment with (a) 0mM, (b) 5mM, and (c) 15mM TMAO. Scale bar=100µm. **B.** The mean intensity of the area of EdU positive cells divided by the mean intensity of total nuclei. *: $p<0.05$, **: $p<0.01$, ****:$p<0.0001$; n=3.

Lastly, stemness was evaluated using the immunocytochemistry assay with anti-SSEA-1 antibody described above. After 5 days of high dose TMAO treatment (0mM, 5mM, 15mM), the cells were stained and imaged. As indicated from Figure 2.9B, no statistically significant differences were found between the control and TMAO-treated groups in terms of cell stemness (% of SSEA-1 positive cells are 98%±2.2 in control vs 94%±1.9 in 5mM, and 94%±2.9 in

15mM, n=3, ns). However, when the high dose treatment was extended to 21 days, there was a significant decrease in SSEA-1 positive cells (% of SSEA-1 positive cells are 96%±1.7 in control vs 93%±3.6 in 1mM, 95%±1.7 in 5mM, and 89%±2.6 in 10mM, n=4, *:p<0.05, **:p<0.001, Figure 2.10B). Thus, high dose TMAO treatment results in decreased mESC viability, proliferation, and stemness.

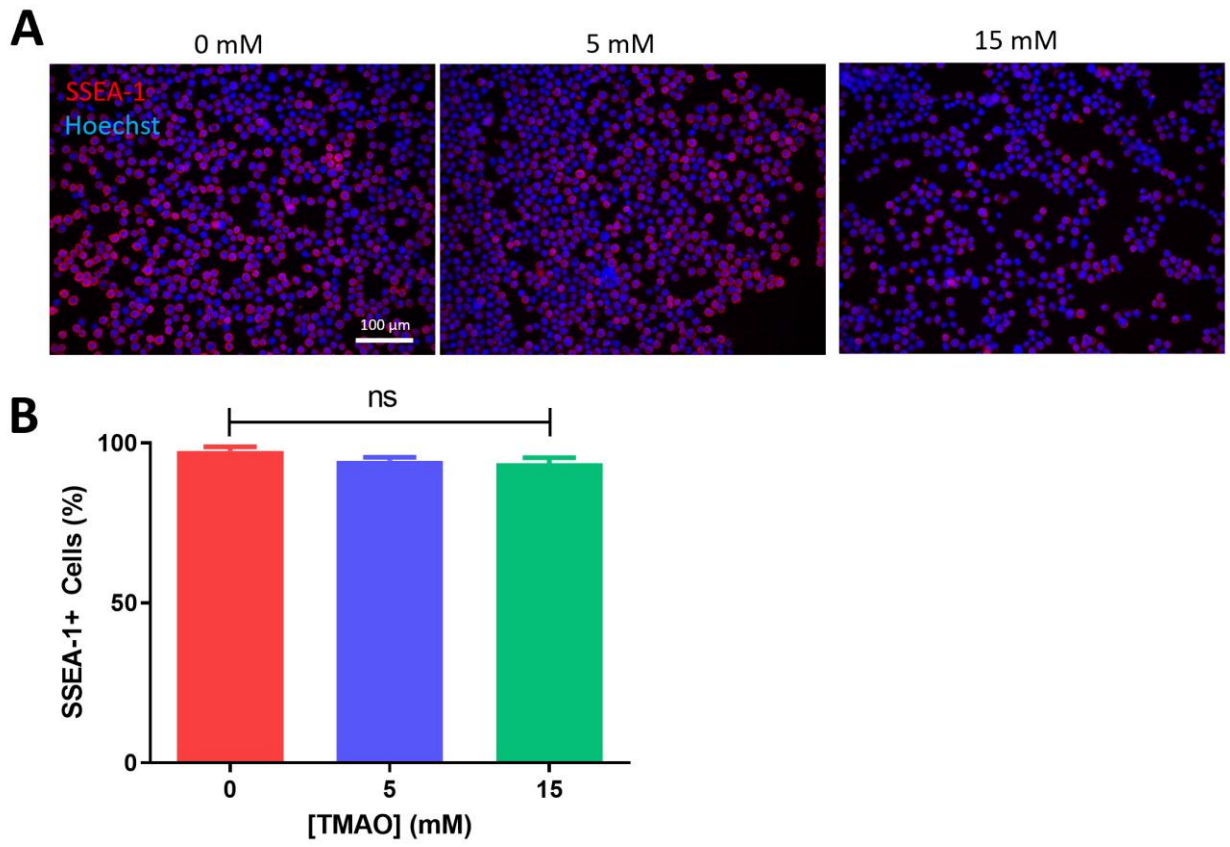

Figure 2.9 mESCs maintain stemness under short-term, high-dose TMAO treatment. **A.** The representative images of mESCs stained with anti-SSEA-1 (red) antibody and Hoechst (blue) after 5 Days of treatment with (a) 0mM, (b) 5mM, and (c) 15mM TMAO. Scale bar=100µm. **B.** The % of SSEA-1 positive cells. ns: not significant; n=3.

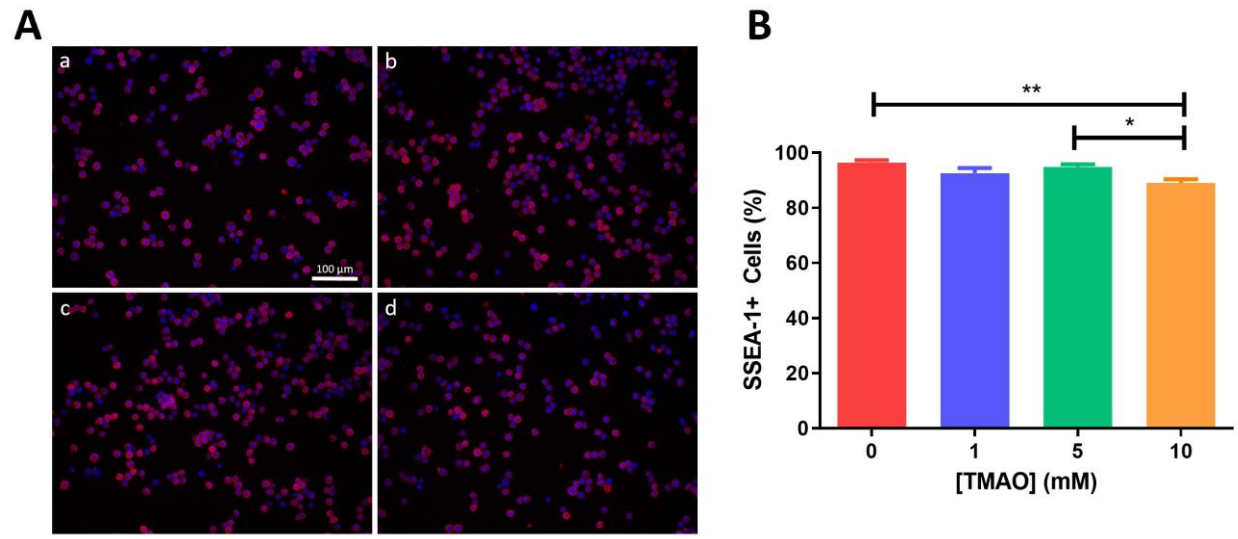

Figure 2.10 mESC stemness decreases under long-term, high-dose TMAO treatment. **A.** The representative images of mESCs stained with anti-SSEA-1 (red) antibody and Hoechst (blue) after 21 Days of treatment with (a) 0mM, (b) 1mM, (c) 5mM, and (d) 10mM TMAO. Scale bar=100µm. **B.** The % of SSEA-1 positive cells. *:$p<0.05$, **: $p<0.01$; n=4.

2.5.3. TMAO Leads to Metabolic Switch from Glycolysis to Oxidative Phosphorylation

As discussed in the introduction, previous studies indicate that TMAO increases ROS generation in several cell types, which disrupts pathways that regulate mitochondrial function and viability, resulting in cell differentiation, senescence, or apoptosis (6, 31, 96). Recently, ROS has been identified as a key regulator of cell potency in pluripotent and multipotent stem cell types (57-59, 79). The greatest source of ROS generation occurs in the mitochondria, and high levels of intracellular ROS indicate the cell is under increased oxidative stress (75). To

investigate whether TMAO may be increasing oxidative stress in embryonic stem cells, as seen in other cell types, we next analyzed the cell's mitochondrial activity after TMAO treatment.

Mitochondrial activity was analyzed using the Seahorse XFe96 Analyzer (for more information on the Seahorse XFe96 Analyzer or Mito Stress Test refer to the methods section). All experiments were carried out in collaboration with Dr. Brown and his student Grace Davis according to published experimental setups (97). Briefly, after 5 days of high dose TMAO treatment (0mM, 5mM, 10mM), mESCs were detached and seeded onto a gelatin-coated XFe96 Cell Culture Microplate (Seahorse Bioscience) at 1e5 cells/well, and allowed 2 hours to attach at 37˚C. This detachment and replating step prior to running experiments was done to ensure the cell number per well was equal across all treatment and control groups.

Glycolytic activity could be analyzed based on extracellular acidification rate (ECAR) measurements after the addition of several different compounds, including glucose, oligomycin, and 2-DG (97). One error in the data occurred in the measurement of baseline ECAR. Consultation with the Agilent Technologies' support team lead us to discover that premature leaking of glucose occurred during baseline ECAR measurements. As a result, baseline ECAR (i.e., Non-Glycolytic Acidification) could not be used in data analysis; however, without the baseline ECAR measurements, we were still able to determine the rate of glycolysis and compensatory glycolysis, based on the tracings shown in Figure 2.11A. Measuring ECAR after the addition of glucose, provides the rate of glycolysis under the different TMAO conditions. The rate of glycolysis decreases significantly with high dose TMAO treatment [ECAR (mpH/min) for rate of glycolysis is 168±18 in control vs 154±22 in 5mM and 139±17 in 10mM, *: $p<0.05$, ****:$p<0.0001$, Figure 2.11B]. Addition of Oligomycin inhibits ATP production through OxPHOS, forcing the cell to compensate with glycolysis for energy production;

therefore, the measurement of ECAR after addition of oligomycin provides the amount of compensatory glycolysis for each TMAO treatment. As shown in Figure 2.11C, the compensatory glycolysis increases significantly with TMAO treatment [ECAR (mpH/min) for compensatory glycolysis is 32±33 in control vs 58±18 in 5mM and 54±518 in 10mM, *: p<0.05, **:p<0.01]. OxPHOS activity could be measured based on oxygen consumption rate (OCR), which was performed in a separate experiment from ECAR measurements. The baseline rate of OCR increased with TMAO treatment [baseline OCR (pmol/min) is 82±15 in control vs 109±17 in 5mM and 93±17 in 10mM, n=3, *: p<0.05, ****:p<0.0001, Figure 2.12B].

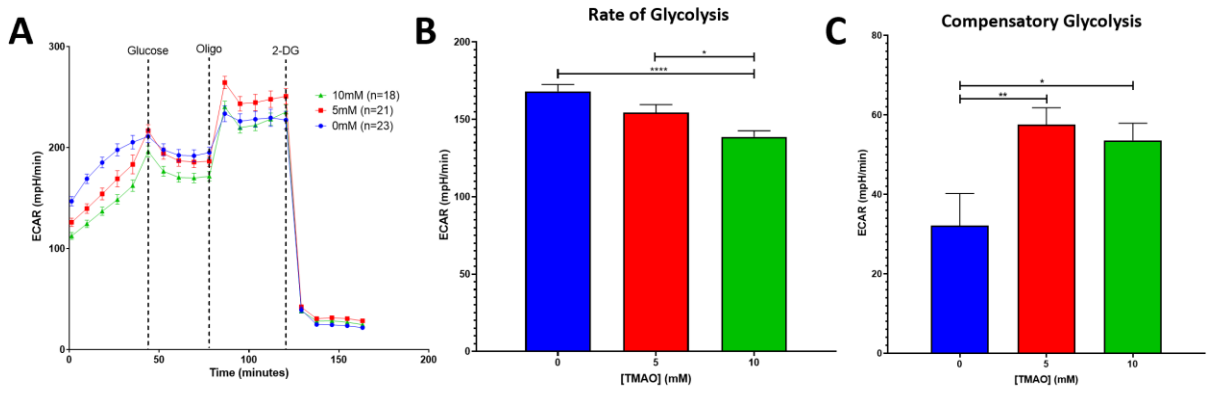

Figure 2.11 Glycolysis stress test. **A.** Extracellular acidification (ECAR) measurements after addition of glucose and oligomycin at different concentrations of TMAO (0mM, 5mM, 10mM). **B.** Baseline rate of glycolysis. **C.** Compensatory glycolysis. *: p<0.05, **: p<0.01, ****: p<0.0001.

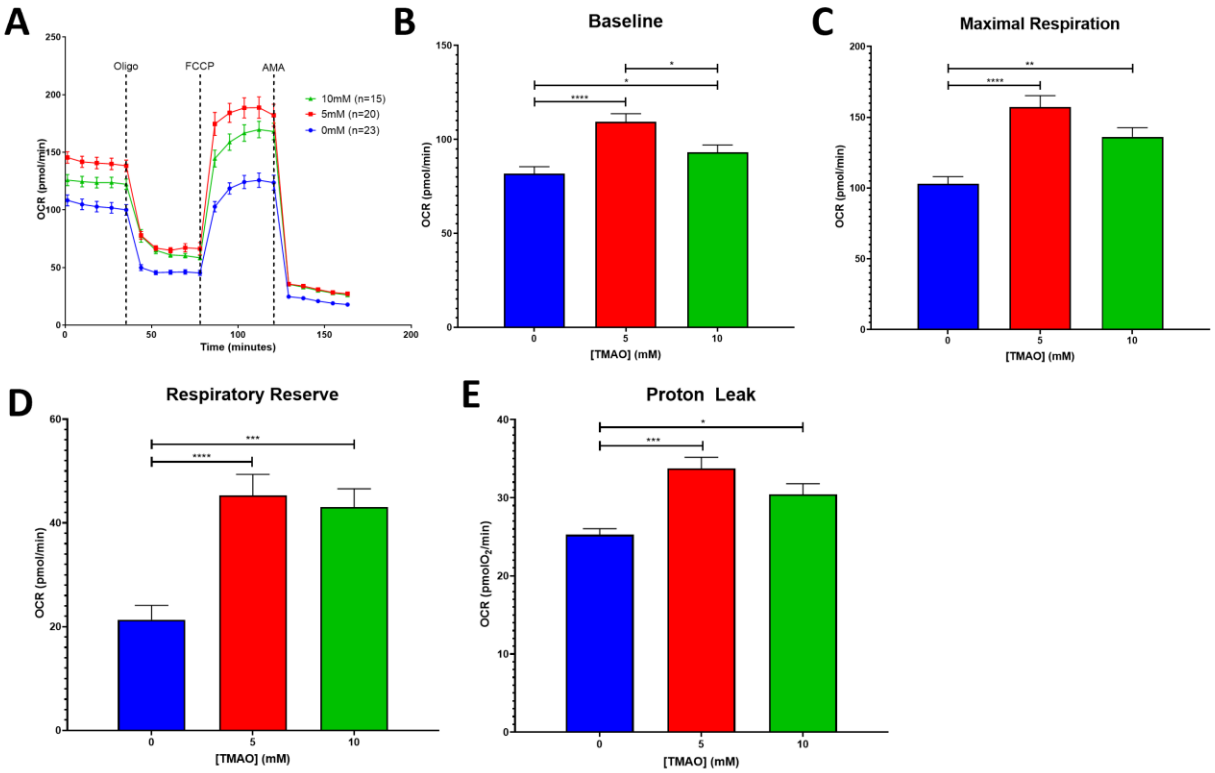

Figure 2.12 Mito stress test. **A.** Oxygen consumption rate (OCR) measurements after addition of oligomycin and FCCP at different concentrations of TMAO (0mM, 5mM, 10mM). **B.** Baseline rate of OCR. **C.** Maximal respiration. **D.** Respiratory reserve. **E.** Proton leak. *: $p<0.05$, **: $p<0.01$, ***: $p<0.001$, ****:$p<0.0001$.

These experiments indicate that the mitochondria of mESCs exposed to high TMAO concentrations exhibit a significant decrease in their ECAR (Figure 2.11B). Notably, when oxidative phosphorylation is shut down with the addition of oligomycin, there is a greater shift to glycolysis in the TMAO-treated cells compared to the control, indicating that the TMAO-treated cells utilize OxPHOS to a greater degree compared to the control (Figure 2.11C). Additionally, the TMAO-treated groups exhibit a significant increase in baseline OCR, compared to the

control (Figure 2.11B). Altogether, these data indicate a metabolic switch from a reliance on glycolysis to OxPHOS. This metabolic switch is required to trigger stem cell differentiation and indicative of loss in stemness (54, 55).

2.5.4. TMAO Increases mESC Respiratory Capacity and Respiratory Reserve

The Seahorse XFe96 Analyzer described above measures respiratory capacity based on oxygen consumption after the addition of FCCP. The compound, FCCP, allows for uninhibited flow of protons across the mitochondrial inner membrane, which results in the cell's maximum OCR. Subtracting non-mitochondrial respiration from the maximal OCR provides a measure of the cell's maximal respiratory capacity. mESCs treated for 5 days with high doses of TMAO exhibited a significant increase in their maximal respiratory capacity [maximal OCR (pmol/min) is 103±20 in control vs 157±31 in 5mM and 136±29 in 10mM, n=3, **: $p<0.01$, ** **:$p<0.0001$, Figure 2.12C]. Additionally, TMAO-treated mESCs also showed a significant increase in their respiratory reserve, which is calculated by subtracting baseline OCR from the maximum respiratory capacity [OCR (pmol/min) for respiratory reserve is 21±11 in control vs 45±15 in 5mM and 43±16 in 10mM, n=3, ***:$p<0.001$, ****:$p<0.0001$, Figure 2.12D]. Altogether, these results indicate that TMAO-treated cells are able to utilize OxPHOS more efficiently compared to the control. This is agrees with papers which demonstrate that a metabolic switch in stem cells is accompanied by an increase in mtDNA content, higher numbers of mitochondria, and more mature mitochondrial cristae (2, 50). Thus, this data provides further confirmation that high dose TMAO treatment may be inducing loss in stemness through modulation of mitochondrial metabolic phenotype.

2.5.5. TMAO Leads to Increase in Proton Leak

The Seahorse XFe96 Analyzer described above measures proton leak based on the rate of oxygen consumption after the addition of oligomycin. The compound, oligomycin, blocks the activity of ATPase, therefore blocking ATP-coupled oxygen consumption. Proton leak is calculated by subtracting non-mitochondrial respiration from the minimum OCR measurement after injection of oligomycin. In other words, proton leak is the measure of oxygen consumption rate after ATPase inhibition with oligomycin. Interestingly, proton leak increased significantly in the TMAO-treated cell groups compared to the control [OCR (pmol/min) for proton leak is 25±3.0 in control vs 34±5.5 in 5mM and 30±6.0 in 10mM, n=3, *:$P<0.05$, ***:$p<0.001$, Figure 2.12E]. This increase in proton leak is associated with increased oxidative stress in several cell types (93, 98). Proton leak is part of a cyto-protective feedback loop in which uncoupler proteins are activated in order to reduce oxidative stress and lower intracellular ROS levels (91, 92, 99, 100). This finding is in agreement with previous *in vitro* studies which demonstrated TMAO lead to an increase in intracellular ROS and subsequent mitochondrial dysfunction (6, 31, 96).

2.6 Discussion

In the present study, we investigated the impact of TMAO on mESC viability, proliferation, and stemness after low dose TMAO treatment to represent physiological conditions and after high dose TMAO treatment to represent diseased conditions. Then, mitochondrial metabolic analysis was performed on mESCs treated with high dose TMAO treatment in order to gain insight into a potential underlying cause for TMAO-induced loss in stemness. The results

show that TMAO does not impact mESC viability, proliferation, or stemness under physiological conditions. This is significant because the pre-implantation blastocyst can be potentially exposed to metabolites such as TMAO through endometrial secretions into the uterus. If TMAO impacted the health of these cells, it may disrupt the process of blastocyst implantation, resulting in loss of the embryo. Additionally, premature differentiation of these cells could be detrimental to proper embryonic and fetal development leading to complications with gestation and with the health of the resulting offspring. After establishing that TMAO does not appear to impact the overall health of mESCs, we next wanted to determine the concentration in which TMAO will have a pathological effect on these cells. We tested several concentrations ranging from 1mM to 30mM TMAO, and found that 5 days of treatment with 5mM and 10mM TMAO resulted in a significant decrease in mESC viability and proliferation. These concentrations have also been used in other in vitro studies with different cell types, including endothelial cells, epithelial cells, and cardiomyocytes (3, 31, 101).

Next, we tested the impact of TMAO on mESC stemness using SSEA-1, a pluripotency marker. When the cells were treated with 5mM and 10mM TMAO for 21 days, the percentage of cells positive for SSEA-1 decreased significantly. This was an interesting finding, because previous studies have shown that TMAO increases ROS generation in several cell types. ROS is an important regulator of potency in stem cells, so this led us to hypothesize that TMAO may be causing a loss in stemness via increased intracellular ROS production. Mitochondria are the greatest sources of ROS in the cell and will produce more ROS under conditions of oxidative stress (75, 102). In order to gain more insight into mitochondrial function of mESCs after TMAO treatment, we used an extracellular flux analyzer to analyze the rate of extracellular acidification (ECAR) and oxygen consumption (OCR), to examine the impact of TMAO on glycolysis and

oxidative phosphorylation, respectively. Interestingly, for cells treated with 5mM and 10mM TMAO for 5 days, we saw a decrease in the rate of glycolysis and an increase in the rate of OxPHOS, along with an increase in compensatory glycolysis once OxPHOS was inhibited. Altogether, these data indicate that TMAO treatment caused the cells to undergo a metabolic switch from glycolysis to OxPHOS.

The metabolic experiments also revealed that TMAO-treated mESCs had higher respiratory capacity and higher respiratory reserve, which further confirms that TMAO promotes a metabolic switch from glycolysis to OxPHOS. Several studies have demonstrated that pluripotent stem cells possess few mitochondria, with poor cristae, and with perinuclear localization (49, 103, 104). As PSCs undergo differentiation, they gradually increase mtDNA content, as well as increase the numbers of mitochondria in the cell. In addition, the mitochondria in differentiated cells are distributed throughout the cytoplasm and have much more mature cristae, which can perform OxPHOS more efficiently (2, 50). These changes are characteristic of a stem cell as it commits to a cell lineage, and switches toward a greater reliance on OxPHOS for metabolic activity. Therefore, the increased respiratory capacity and respiratory reserve observed in TMAO-treated mESCs indicates these cells are increasing their capacity to perform OxpHOS in order to support a new metabolic phenotype and promote differentiation.

Additionally, mESCs which received the high dose TMAO treatment condition exhibited an increase in proton leak, which is an indicator of oxidative stress. When cells are under oxidative stress, they generate higher amounts of ROS from the ETC (75, 102). In order to combat the higher ROS levels, mESCs express uncoupler protein 2 (UCP2), which has several functions important for maintaining cellular redox balance. One function is to uncouple oxygen consumption with ATP production in order to lower the mitochondrial membrane potential,

which is demonstrated in our results where oxygen continues to be consumed even after ATPase has been inhibited by oligomycin. Although this mechanism results in loss of ATP production, it is an important mechanism in stem cells for lowering ETC activity, and thus minimizing ROS production (90-92) Another function of UCP2 is to impair glucose oxidation and shunt pyruvate toward glycolysis. This increases glycolytic flux and lowers ETC activity, which greatly reduces ROS production (50, 54).

mESCs are highly sensitive to ROS, as are most stem cell types, because ROS acts as a regulator of potency (58, 79, 81). A metabolic switch from glycolysis to OxPHOS as well as an increase in ROS generation are required for the onset of differentiation in mESCs and other stem cell types (50, 54, 55). As a result, stem cells have several mechanisms in place in order to tightly regulate their metabolic phenotype and cellular redox balance (62, 76). In fact, recent studies have uncovered the complex interplay between pathways which regulate metabolism and those that regulate potency, demonstrating that the metabolic phenotype of stem cells is influenced by pluripotency factors, and also pluripotency factors may modulate the metabolic phenotype (1, 2). Therefore, based on the data from this study it appears that TMAO may be modulating stem cell properties through alteration of the cell's metabolic activity. Further research is required to elucidate the exact underlying mechanism; however, our data indicates that TMAO-induced proton leak in mESCs may be caused by increased oxidative stress, which in turn causes a metabolic switch toward OxPHOS, triggering the onset of differentiation and subsequent loss of mESC stemness.

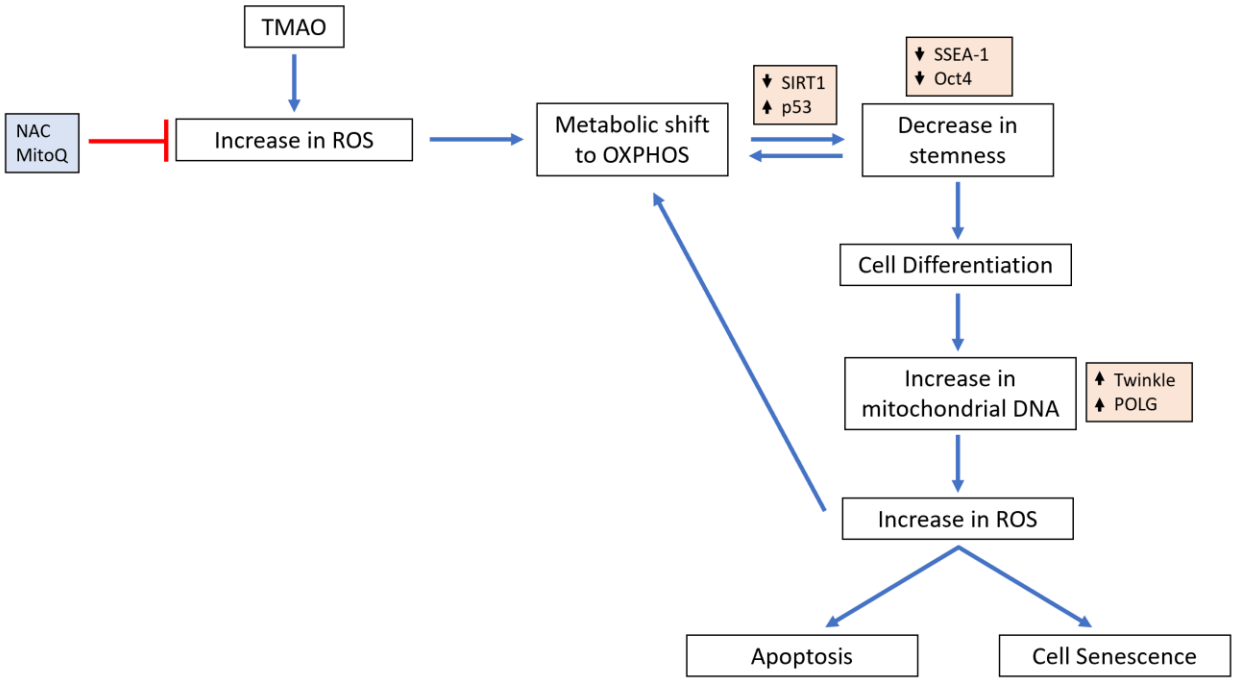

Figure 2.13 The proposed mechanism.

3. CHAPTER THREE: OVERALL CONCLUSIONS AND FUTURE WORK

3.1. Overall Conclusions

In this study we provide evidence that TMAO does not negatively impact mESCs of the early embryo, since long-term treatment with physiological concentrations of TMAO did not negatively impact mESC viability, proliferation, and stemness. However, under high dose TMAO treatment conditions, TMAO significantly reduced mESC viability, proliferation, stemness, and altered mESC metabolic activity. These negative impacts that result from high TMAO concentrations provide insight into the potential impact of sustained high plasma TMAO levels on adult stem cell populations, which are exposed to TMAO throughout the entire human life span. The dietary precursors for TMAO are a staple of the American diet, and the data from this project suggest that TMAO may contribute to stem cell exhaustion and thus the onset of chronic and age-related diseases. Future studies are required to further examine the underlying mechanism by which TMAO effects mESCs as well as the potential impact TMAO may have on the different potent cell types present in adult tissues which have been subjected to a lifetime of high TMAO exposure.

3.2. Future Work

The long-term goal of this project is to understand the underlying mechanism by which TMAO modulates mESC metabolic activity and pluripotent pathways, and to explore potential therapeutic strategies for TMAO-induced cellular abnormalities. The current studies only provide a potential mechanism, and more extensive studies must be done to validate the mechanism proposed in Figure 2.13. The proposed work would include, but is not limited to:

1) Measure UCP2 expression in mESCs under the different TMAO conditions:

UCP2 plays an important role in maintaining pluripotency and is repressed during the onset of differentiation. UCP2 functions to reduce ROS generation and maintain high glycolytic flux, potentially through increased proton leak in the ETC. In my project, I observed that TMAO treatment significantly increased proton leak. Future studies should confirm whether UCP2 expression is increased under TMAO treatment to help determine whether TMAO induces oxidative stress and excessive ROS generation in mESCs.

2) Measure intracellular ROS:

Intracellular ROS measurement is required to confirm TMAO indeed increases ROS generation in mESCs, which is indicated by increased proton leak and by previous studies conducted in various cell types. I attempted to measure intracellular ROS with two different methods: DCDFA dye and a fluorometric H_2O_2 assay kit. Neither of these methods were able to produce accurate intracellular ROS levels, perhaps because these methods are not compatible with mESCs. An alternative would be to examine the expression of genes regulating oxidative stress, including *SOD1*, *SOD2*, and *CAT* (gene for catalase expression).

3) Measure TWINKLE and POLG expression:

TWINKLE is the mtDNA-specific helicase and polymerase gamma A (POLGA) is the mitochondrial-specific DNA polymerase. These proteins were measured in other studies to confirm an increase in mtDNA replication during the onset of differentiation (51, 105). My

data indicates that TMAO-induces a loss in mESC pluripotency, which would be confirmed by the increase in expression of proteins involved in mtDNA replication.

4) Measure expression of SIRT1, p53, and *Nanog*:

   As discussed in Section 1.7.2., SIRT1 is responsible for inhibiting p53 suppression of Nanog gene expression. However, in situations of high oxidative stress, SIRT1 is suppressed and p53 is upregulated, resulting in downregulation of core pluripotency factors (e.g., NANOG, OCT4, SOX2) (79). Moreover, there is also a strong possibility that DNA damage will cause p53-induced premature differentiation of certain adult stem cell types (36, 106). Therefore, the measurement of these proteins may help to elucidate a potential pathway which links TMAO-induced oxidative stress to loss of potency in mESCs and other stem cell types.

5) Determine whether antioxidant treatment with NAC and MitoQ can rescue TMAO-induced negative effects:

   Several studies have demonstrated the ability of antioxidants to reverse the negative effects of TMAO on different cell types. Figure 1.4 shows that treatment with NAC and MitoQ were able to block ROS from downregulating NANOG gene expression via the SIRT1-p53 pathway. If TMAO indeed induces loss of pluripotency via induction of oxidative stress, then NAC and MitoQ may be effective treatments.

REFERENCES

1. Mathieu J, Ruohola-Baker H. Metabolic remodeling during the loss and acquisition of pluripotency. Development. 2017;144(4):541-51.
2. Shyh-Chang N, Daley GQ, Cantley LC. Stem cell metabolism in tissue development and aging. Development. 2013;140(12):2535-47.
3. Ke Y, Li D, Zhao M, Liu C, Liu J, Zeng A, et al. Gut flora-dependent metabolite Trimethylamine-N-oxide accelerates endothelial cell senescence and vascular aging through oxidative stress. Free Radic Biol Med. 2018;116:88-100.
4. Koeth RA, Wang Z, Levison BS, Buffa JA, Org E, Sheehy BT, et al. Intestinal microbiota metabolism of L-carnitine, a nutrient in red meat, promotes atherosclerosis. Nat Med. 2013;19(5):576-85.
5. Wang Z, Klipfell E, Bennett BJ, Koeth R, Levison BS, Dugar B, et al. Gut flora metabolism of phosphatidylcholine promotes cardiovascular disease. Nature. 2011;472(7341):57-63.
6. Li D, Ke Y, Zhan R, Liu C, Zhao M, Zeng A, et al. Trimethylamine-N-oxide promotes brain aging and cognitive impairment in mice. Aging Cell. 2018;17(4):e12768.
7. Seldin MM, Meng Y, Qi H, Zhu W, Wang Z, Hazen SL, et al. Trimethylamine N-Oxide Promotes Vascular Inflammation Through Signaling of Mitogen-Activated Protein Kinase and Nuclear Factor-kappaB. J Am Heart Assoc. 2016;5(2).
8. Yancey PH. Organic osmolytes as compatible, metabolic and counteracting cytoprotectants in high osmolarity and other stresses. J Exp Biol. 2005;208(Pt 15):2819-30.
9. Bennion BJ, Daggett V. Counteraction of urea-induced protein denaturation by trimethylamine N-oxide: a chemical chaperone at atomic resolution. Proc Natl Acad Sci U S A. 2004;101(17):6433-8.
10. Sharp KAM, Bhupinder; Manas, Eric; Vanderkooi, Jane M. Structure Changes Induced by Hydrophobic and Polar Solutes Revealed by Simulations and Infrared Spectroscopy. The Journal of Chemical Physics. 2001;114(4):1791-6.
11. Miller CA, Corbin KD, da Costa KA, Zhang S, Zhao X, Galanko JA, et al. Effect of egg ingestion on trimethylamine-N-oxide production in humans: a randomized, controlled, dose-response study. Am J Clin Nutr. 2014;100(3):778-86.
12. Romano KA, Vivas EI, Amador-Noguez D, Rey FE. Intestinal microbiota composition modulates choline bioavailability from diet and accumulation of the proatherogenic metabolite trimethylamine-N-oxide. mBio. 2015;6(2):e02481.
13. Tang WH, Wang Z, Levison BS, Koeth RA, Britt EB, Fu X, et al. Intestinal microbial metabolism of phosphatidylcholine and cardiovascular risk. N Engl J Med. 2013;368(17):1575-84.
14. Cho CE, Taesuwan S, Malysheva OV, Bender E, Tulchinsky NF, Yan J, et al. Trimethylamine-N-oxide (TMAO) response to animal source foods varies among healthy young men and is influenced by their gut microbiota composition: A randomized controlled trial. Mol Nutr Food Res. 2017;61(1).
15. Hartiala J, Bennett BJ, Tang WH, Wang Z, Stewart AF, Roberts R, et al. Comparative genome-wide association studies in mice and humans for trimethylamine N-oxide, a proatherogenic metabolite of choline and L-carnitine. Arterioscler Thromb Vasc Biol. 2014;34(6):1307-13.

16. Wang Z, Levison BS, Hazen JE, Donahue L, Li XM, Hazen SL. Measurement of trimethylamine-N-oxide by stable isotope dilution liquid chromatography tandem mass spectrometry. Anal Biochem. 2014;455:35-40.
17. Missailidis C, Hallqvist J, Qureshi AR, Barany P, Heimburger O, Lindholm B, et al. Serum Trimethylamine-N-Oxide Is Strongly Related to Renal Function and Predicts Outcome in Chronic Kidney Disease. PLoS One. 2016;11(1):e0141738.
18. Kaysen GA, Johansen KL, Chertow GM, Dalrymple LS, Kornak J, Grimes B, et al. Associations of Trimethylamine N-Oxide With Nutritional and Inflammatory Biomarkers and Cardiovascular Outcomes in Patients New to Dialysis. J Ren Nutr. 2015;25(4):351-6.
19. Tang WH, Wang Z, Fan Y, Levison B, Hazen JE, Donahue LM, et al. Prognostic value of elevated levels of intestinal microbe-generated metabolite trimethylamine-N-oxide in patients with heart failure: refining the gut hypothesis. J Am Coll Cardiol. 2014;64(18):1908-14.
20. Dambrova M, Latkovskis G, Kuka J, Strele I, Konrade I, Grinberga S, et al. Diabetes is Associated with Higher Trimethylamine N-oxide Plasma Levels. Exp Clin Endocrinol Diabetes. 2016;124(4):251-6.
21. Lever M, George PM, Slow S, Bellamy D, Young JM, Ho M, et al. Betaine and Trimethylamine-N-Oxide as Predictors of Cardiovascular Outcomes Show Different Patterns in Diabetes Mellitus: An Observational Study. PLoS One. 2014;9(12):e114969.
22. Del Rio D, Zimetti F, Caffarra P, Tassotti M, Bernini F, Brighenti F, et al. The Gut Microbial Metabolite Trimethylamine-N-Oxide Is Present in Human Cerebrospinal Fluid. Nutrients. 2017;9(10).
23. Vogt NM, Romano KA, Darst BF, Engelman CD, Johnson SC, Carlsson CM, et al. The gut microbiota-derived metabolite trimethylamine N-oxide is elevated in Alzheimer's disease. Alzheimers Res Ther. 2018;10(1):124.
24. Nie J, Xie L, Zhao BX, Li Y, Qiu B, Zhu F, et al. Serum Trimethylamine N-Oxide Concentration Is Positively Associated With First Stroke in Hypertensive Patients. Stroke. 2018;49(9):2021-8.
25. Stubbs JR, House JA, Ocque AJ, Zhang S, Johnson C, Kimber C, et al. Serum Trimethylamine-N-Oxide is Elevated in CKD and Correlates with Coronary Atherosclerosis Burden. J Am Soc Nephrol. 2016;27(1):305-13.
26. Velasquez MT, Ramezani A, Manal A, Raj DS. Trimethylamine N-Oxide: The Good, the Bad and the Unknown. Toxins (Basel). 2016;8(11).
27. Fogelman AM. TMAO is both a biomarker and a renal toxin. Circ Res. 2015;116(3):396-7.
28. Geng J, Yang C, Wang B, Zhang X, Hu T, Gu Y, et al. Trimethylamine N-oxide promotes atherosclerosis via CD36-dependent MAPK/JNK pathway. Biomed Pharmacother. 2018;97:941-7.
29. Chen ML, Zhu XH, Ran L, Lang HD, Yi L, Mi MT. Trimethylamine-N-Oxide Induces Vascular Inflammation by Activating the NLRP3 Inflammasome Through the SIRT3-SOD2-mtROS Signaling Pathway. J Am Heart Assoc. 2017;6(9).
30. Ma G, Pan B, Chen Y, Guo C, Zhao M, Zheng L, et al. Trimethylamine N-oxide in atherogenesis: impairing endothelial self-repair capacity and enhancing monocyte adhesion. Biosci Rep. 2017;37(2).

31. Chou RH, Chen CY, Chen IC, Huang HL, Lu YW, Kuo CS, et al. Trimethylamine N-Oxide, Circulating Endothelial Progenitor Cells, and Endothelial Function in Patients with Stable Angina. Sci Rep. 2019;9(1):4249.
32. Brons IG, Smithers LE, Trotter MW, Rugg-Gunn P, Sun B, Chuva de Sousa Lopes SM, et al. Derivation of pluripotent epiblast stem cells from mammalian embryos. Nature. 2007;448(7150):191-5.
33. Nichols J, Smith A. Naive and primed pluripotent states. Cell Stem Cell. 2009;4(6):487-92.
34. Zhou W, Choi M, Margineantu D, Margaretha L, Hesson J, Cavanaugh C, et al. HIF1alpha induced switch from bivalent to exclusively glycolytic metabolism during ESC-to-EpiSC/hESC transition. EMBO J. 2012;31(9):2103-16.
35. Stambrook PJ, Tichy ED. Preservation of genomic integrity in mouse embryonic stem cells. Adv Exp Med Biol. 2010;695:59-75.
36. Xu Y. A new role for p53 in maintaining genetic stability in embryonic stem cells. Cell Cycle. 2005;4(3):363-4.
37. Cervantes RB, Stringer JR, Shao C, Tischfield JA, Stambrook PJ. Embryonic stem cells and somatic cells differ in mutation frequency and type. Proc Natl Acad Sci U S A. 2002;99(6):3586-90.
38. Hill MA. Mouse Timeline Detailed 2020 [Available from: https://embryology.med.unsw.edu.au/embryology/index.php/Main_Page.
39. Amoroso EC. Placentation. 3 ed. Parkes AS, editor: London: Longmans, Green; 1952.
40. McRae AC, Church RB. Cytoplasmic projections of trophectoderm distinguish implanting from preimplanting and implantation-delayed mouse blastocytes. J Reprod Fertil. 1990;88(1):31-40.
41. Wolter J. The Process of Implantation of Embryos in Primates. Embryo Project Encyclopedia: Arizona State University. School of Life Sciences. Center for Biology and Society. Embryo Project Encyclopedia.; 2013.
42. Kim SM, Kim JS. A Review of Mechanisms of Implantation. Dev Reprod. 2017;21(4):351-9.
43. Johnson MT, Mahmood S, Patel MS. Intermediary metabolism and energetics during murine early embryogenesis. J Biol Chem. 2003;278(34):31457-60.
44. Condic ML. Totipotency: what it is and what it is not. Stem Cells Dev. 2014;23(8):796-812.
45. Li L, Clevers H. Coexistence of quiescent and active adult stem cells in mammals. Science. 2010;327(5965):542-5.
46. Chen T, Wang F, Wu M, Wang ZZ. Development of hematopoietic stem and progenitor cells from human pluripotent stem cells. J Cell Biochem. 2015;116(7):1179-89.
47. Martínez MG, A.; Luzardo, E.; Chávez-Castillo, M.; Olivar, LC.; Salazar, J.; Velasco, M.; Quintero, JJR; Bermúdez, V. Energetic metabolism in cardiomyocytes: molecular basis of heart ischemia and arrhythmogenesis. Vessel Plus. 2017(1):130-41.
48. Vander Heiden MG, Cantley LC, Thompson CB. Understanding the Warburg effect: the metabolic requirements of cell proliferation. Science. 2009;324(5930):1029-33.
49. Van Blerkom J. Mitochondria in early mammalian development. Semin Cell Dev Biol. 2009;20(3):354-64.

50. Zhang J, Khvorostov I, Hong JS, Oktay Y, Vergnes L, Nuebel E, et al. UCP2 regulates energy metabolism and differentiation potential of human pluripotent stem cells. EMBO J. 2011;30(24):4860-73.
51. Facucho-Oliveira JM, Alderson J, Spikings EC, Egginton S, St John JC. Mitochondrial DNA replication during differentiation of murine embryonic stem cells. J Cell Sci. 2007;120(Pt 22):4025-34.
52. Leese HJ, Barton AM. Pyruvate and glucose uptake by mouse ova and preimplantation embryos. J Reprod Fertil. 1984;72(1):9-13.
53. Filosa S, Fico A, Paglialunga F, Balestrieri M, Crooke A, Verde P, et al. Failure to increase glucose consumption through the pentose-phosphate pathway results in the death of glucose-6-phosphate dehydrogenase gene-deleted mouse embryonic stem cells subjected to oxidative stress. Biochem J. 2003;370(Pt 3):935-43.
54. Moussaieff A, Rouleau M, Kitsberg D, Cohen M, Levy G, Barasch D, et al. Glycolysis-mediated changes in acetyl-CoA and histone acetylation control the early differentiation of embryonic stem cells. Cell Metab. 2015;21(3):392-402.
55. Shyh-Chang N, Daley GQ. Metabolic switches linked to pluripotency and embryonic stem cell differentiation. Cell Metab. 2015;21(3):349-50.
56. Pattappa G, Thorpe SD, Jegard NC, Heywood HK, de Bruijn JD, Lee DA. Continuous and uninterrupted oxygen tension influences the colony formation and oxidative metabolism of human mesenchymal stem cells. Tissue Eng Part C Methods. 2013;19(1):68-79.
57. Renault VM, Rafalski VA, Morgan AA, Salih DA, Brett JO, Webb AE, et al. FoxO3 regulates neural stem cell homeostasis. Cell Stem Cell. 2009;5(5):527-39.
58. Tothova Z, Kollipara R, Huntly BJ, Lee BH, Castrillon DH, Cullen DE, et al. FoxOs are critical mediators of hematopoietic stem cell resistance to physiologic oxidative stress. Cell. 2007;128(2):325-39.
59. Chen CT, Shih YR, Kuo TK, Lee OK, Wei YH. Coordinated changes of mitochondrial biogenesis and antioxidant enzymes during osteogenic differentiation of human mesenchymal stem cells. Stem Cells. 2008;26(4):960-8.
60. Suda T, Takubo K, Semenza GL. Metabolic regulation of hematopoietic stem cells in the hypoxic niche. Cell Stem Cell. 2011;9(4):298-310.
61. Chung S, Dzeja PP, Faustino RS, Perez-Terzic C, Behfar A, Terzic A. Mitochondrial oxidative metabolism is required for the cardiac differentiation of stem cells. Nat Clin Pract Cardiovasc Med. 2007;4 Suppl 1:S60-7.
62. Heilig C, Brosius F, Siu B, Concepcion L, Mortensen R, Heilig K, et al. Implications of glucose transporter protein type 1 (GLUT1)-haplodeficiency in embryonic stem cells for their survival in response to hypoxic stress. Am J Pathol. 2003;163(5):1873-85.
63. Yu L, Ji KY, Zhang J, Xu Y, Ying Y, Mai T, et al. Core pluripotency factors promote glycolysis of human embryonic stem cells by activating GLUT1 enhancer. Protein Cell. 2019;10(9):668-80.
64. Kim H, Jang H, Kim TW, Kang BH, Lee SE, Jeon YK, et al. Core Pluripotency Factors Directly Regulate Metabolism in Embryonic Stem Cell to Maintain Pluripotency. Stem Cells. 2015;33(9):2699-711.
65. Cao Y, Guo WT, Tian S, He X, Wang XW, Liu X, et al. miR-290/371-Mbd2-Myc circuit regulates glycolytic metabolism to promote pluripotency. EMBO J. 2015;34(5):609-23.

66. Meshorer E, Misteli T. Chromatin in pluripotent embryonic stem cells and differentiation. Nat Rev Mol Cell Biol. 2006;7(7):540-6.
67. Saraiva NZ, Oliveira CS, Garcia JM. Histone acetylation and its role in embryonic stem cell differentiation. World J Stem Cells. 2010;2(6):121-6.
68. Wang J, Alexander P, Wu L, Hammer R, Cleaver O, McKnight SL. Dependence of mouse embryonic stem cells on threonine catabolism. Science. 2009;325(5939):435-9.
69. Shyh-Chang N, Locasale JW, Lyssiotis CA, Zheng Y, Teo RY, Ratanasirintrawoot S, et al. Influence of threonine metabolism on S-adenosylmethionine and histone methylation. Science. 2013;339(6116):222-6.
70. Wellen KE, Hatzivassiliou G, Sachdeva UM, Bui TV, Cross JR, Thompson CB. ATP-citrate lyase links cellular metabolism to histone acetylation. Science. 2009;324(5930):1076-80.
71. Tahiliani M, Koh KP, Shen Y, Pastor WA, Bandukwala H, Brudno Y, et al. Conversion of 5-methylcytosine to 5-hydroxymethylcytosine in mammalian DNA by MLL partner TET1. Science. 2009;324(5929):930-5.
72. Loh YH, Zhang W, Chen X, George J, Ng HH. Jmjd1a and Jmjd2c histone H3 Lys 9 demethylases regulate self-renewal in embryonic stem cells. Genes Dev. 2007;21(20):2545-57.
73. Carey BW, Finley LW, Cross JR, Allis CD, Thompson CB. Intracellular alpha-ketoglutarate maintains the pluripotency of embryonic stem cells. Nature. 2015;518(7539):413-6.
74. Hwang IY, Kwak S, Lee S, Kim H, Lee SE, Kim JH, et al. Psat1-Dependent Fluctuations in alpha-Ketoglutarate Affect the Timing of ESC Differentiation. Cell Metab. 2016;24(3):494-501.
75. Turrens JF. Mitochondrial formation of reactive oxygen species. J Physiol. 2003;552(Pt 2):335-44.
76. Perales-Clemente E, Folmes CD, Terzic A. Metabolic regulation of redox status in stem cells. Antioxid Redox Signal. 2014;21(11):1648-59.
77. Wiseman H, Halliwell B. Damage to DNA by reactive oxygen and nitrogen species: role in inflammatory disease and progression to cancer. Biochem J. 1996;313 (Pt 1):17-29.
78. Grune T, Reinheckel T, Davies KJ. Degradation of oxidized proteins in mammalian cells. FASEB J. 1997;11(7):526-34.
79. Han MK, Song EK, Guo Y, Ou X, Mantel C, Broxmeyer HE. SIRT1 regulates apoptosis and Nanog expression in mouse embryonic stem cells by controlling p53 subcellular localization. Cell Stem Cell. 2008;2(3):241-51.
80. Hong H, Takahashi K, Ichisaka T, Aoi T, Kanagawa O, Nakagawa M, et al. Suppression of induced pluripotent stem cell generation by the p53-p21 pathway. Nature. 2009;460(7259):1132-5.
81. Lin T, Chao C, Saito S, Mazur SJ, Murphy ME, Appella E, et al. p53 induces differentiation of mouse embryonic stem cells by suppressing Nanog expression. Nat Cell Biol. 2005;7(2):165-71.
82. He H, Wang C, Dai Q, Li F, Bergholz J, Li Z, et al. p53 and p73 Regulate Apoptosis but Not Cell-Cycle Progression in Mouse Embryonic Stem Cells upon DNA Damage and Differentiation. Stem Cell Reports. 2016;7(6):1087-98.
83. Lin T, Lin Y. p53 switches off pluripotency on differentiation. Stem Cell Res Ther. 2017;8(1):44.

84. Chae HD, Broxmeyer HE. SIRT1 deficiency downregulates PTEN/JNK/FOXO1 pathway to block reactive oxygen species-induced apoptosis in mouse embryonic stem cells. Stem Cells Dev. 2011;20(7):1277-85.
85. Li H. Sirtuin 1 (SIRT1) and Oxidative Stress. Systems Biology of Free Radicals and Antioxidants. 2014:417-35.
86. Lee J, Cho YS, Jung H, Choi I. Pharmacological Regulation of Oxidative Stress in Stem Cells. Oxid Med Cell Longev. 2018;2018:4081890.
87. Solari C, Petrone MV, Vazquez Echegaray C, Cosentino MS, Waisman A, Francia M, et al. Superoxide dismutase 1 expression is modulated by the core pluripotency transcription factors Oct4, Sox2 and Nanog in embryonic stem cells. Mech Dev. 2018;154:116-21.
88. Zhang X, Yalcin S, Lee DF, Yeh TY, Lee SM, Su J, et al. FOXO1 is an essential regulator of pluripotency in human embryonic stem cells. Nat Cell Biol. 2011;13(9):1092-9.
89. Rupprecht A, Sittner D, Smorodchenko A, Hilse KE, Goyn J, Moldzio R, et al. Uncoupling protein 2 and 4 expression pattern during stem cell differentiation provides new insight into their putative function. PLoS One. 2014;9(2):e88474.
90. Mattiasson G, Shamloo M, Gido G, Mathi K, Tomasevic G, Yi S, et al. Uncoupling protein-2 prevents neuronal death and diminishes brain dysfunction after stroke and brain trauma. Nat Med. 2003;9(8):1062-8.
91. Negre-Salvayre A, Hirtz C, Carrera G, Cazenave R, Troly M, Salvayre R, et al. A role for uncoupling protein-2 as a regulator of mitochondrial hydrogen peroxide generation. FASEB J. 1997;11(10):809-15.
92. Echtay KS. Mitochondrial uncoupling proteins--what is their physiological role? Free Radic Biol Med. 2007;43(10):1351-71.
93. Zhao RZ, Jiang S, Zhang L, Yu ZB. Mitochondrial electron transport chain, ROS generation and uncoupling (Review). Int J Mol Med. 2019;44(1):3-15.
94. Divakaruni AS, Rogers GW, Murphy AN. Measuring Mitochondrial Function in Permeabilized Cells Using the Seahorse XF Analyzer or a Clark-Type Oxygen Electrode. Curr Protoc Toxicol. 2014;60:25 2 1-16.
95. Tamm C, Pijuan Galito S, Anneren C. A comparative study of protocols for mouse embryonic stem cell culturing. PLoS One. 2013;8(12):e81156.
96. Sun X, Jiao X, Ma Y, Liu Y, Zhang L, He Y, et al. Trimethylamine N-oxide induces inflammation and endothelial dysfunction in human umbilical vein endothelial cells via activating ROS-TXNIP-NLRP3 inflammasome. Biochem Biophys Res Commun. 2016;481(1-2):63-70.
97. McDaniel DK, Ringel-Scaia VM, Morrison HA, Coutermarsh-Ott S, Council-Troche M, Angle JW, et al. Pulmonary Exposure to Magneli Phase Titanium Suboxides Results in Significant Macrophage Abnormalities and Decreased Lung Function. Front Immunol. 2019;10:2714.
98. Cheng J, Nanayakkara G, Shao Y, Cueto R, Wang L, Yang WY, et al. Mitochondrial Proton Leak Plays a Critical Role in Pathogenesis of Cardiovascular Diseases. Adv Exp Med Biol. 2017;982:359-70.
99. Valle A, Oliver J, Roca P. Role of uncoupling proteins in cancer. Cancers (Basel). 2010;2(2):567-91.

100. Echtay KS, Murphy MP, Smith RA, Talbot DA, Brand MD. Superoxide activates mitochondrial uncoupling protein 2 from the matrix side. Studies using targeted antioxidants. J Biol Chem. 2002;277(49):47129-35.
101. Oakley C. The Direct Inotropic and Chronotropic Effects of Trimethylamine-N-Oxide on Cardiac Muscle: University of Kansas; 2018.
102. Korshunov SS, Skulachev VP, Starkov AA. High protonic potential actuates a mechanism of production of reactive oxygen species in mitochondria. FEBS Lett. 1997;416(1):15-8.
103. Baharvand H, Matthaei KI. The ultrastructure of mouse embryonic stem cells. Reprod Biomed Online. 2003;7(3):330-5.
104. Prigione A, Fauler B, Lurz R, Lehrach H, Adjaye J. The senescence-related mitochondrial/oxidative stress pathway is repressed in human induced pluripotent stem cells. Stem Cells. 2010;28(4):721-33.
105. Dickinson A, Yeung KY, Donoghue J, Baker MJ, Kelly RD, McKenzie M, et al. The regulation of mitochondrial DNA copy number in glioblastoma cells. Cell Death Differ. 2013;20(12):1644-53.
106. Jain AK, Barton MC. p53: emerging roles in stem cells, development and beyond. Development. 2018;145(8).